AGU ADVANCING EARTH AND SPACE SCIENCE

Water Resources Research

RESEARCH ARTICLE
10.1029/2020WR029170

Dynamic Hillslope Soil Moisture in a Mediterranean Montane Watershed

Salli F. Dymond[1], Joseph W. Wagenbrenner[2], Elizabeth T. Keppeler[3], and Kevin D. Bladon[4]

[1]Department of Earth and Environmental Sciences, University of Minnesota Duluth, Duluth, MN, USA, [2]USDA Forest Service, Pacific Southwest Research Station, Arcata, CA, USA, [3]USDA Forest Service, Pacific Southwest Research Station, Fort Bragg, CA, USA, [4]Department of Forest Engineering, Resources, and Management, Oregon State University, Corvallis, OR, USA

Key Points:

- Seasonal soil moisture largely manifested into relative wet and dry states
- Counter to our expectations, ridgetops remained one of the wettest topographic positions on the landscape during the wet season
- There was greater homogeneity in dry season soil moisture along the hillslopes

Supporting Information:

Supporting Information may be found in the online version of this article.

Correspondence to:

S. F. Dymond,
sdymond@d.umn.edu

Citation:

Dymond, S. F., Wagenbrenner, J. W., Keppeler, E. T., & Bladon, K. D. (2021). Dynamic hillslope soil moisture in a Mediterranean montane watershed. *Water Resources Research*, *57*, e2020WR029170. https://doi.org/10.1029/2020WR029170

Received 11 NOV 2020
Accepted 27 OCT 2021

Author Contributions:

Conceptualization: Salli F. Dymond, Elizabeth T. Keppeler, Kevin D. Bladon
Formal analysis: Salli F. Dymond
Investigation: Joseph W. Wagenbrenner, Elizabeth T. Keppeler, Kevin D. Bladon
Methodology: Salli F. Dymond, Elizabeth T. Keppeler, Kevin D. Bladon
Project Administration: Joseph W. Wagenbrenner
Supervision: Joseph W. Wagenbrenner, Elizabeth T. Keppeler
Writing – original draft: Salli F. Dymond
Writing – review & editing: Salli F. Dymond, Joseph W. Wagenbrenner, Elizabeth T. Keppeler, Kevin D. Bladon

Abstract Variations in hillslope soil moisture control forest hydrologic fluxes and storage pools, yet sparse observations combined with the complexity and heterogeneity of water movement and storage in the vadose zone can make temporal and spatial patterns and processes difficult to predict. We used two years of field observations of volumetric soil moisture at three depths (15, 30, and 100 cm) across five topographic positions (riparian, toeslope, sideslope, shoulder, and ridge) along three hillslope transects to better understand how soil moisture changes with hillslope position and through time. As expected, we found higher values of soil moisture at all depths at the riparian and toeslope positions. Unexpectedly, we found that ridges were particularly wet during the wet winter months and dried quickly during the summer months, indicating that topography alone cannot account for mean wet season soil moisture in our Mediterranean climate field site. The variability in soil moisture across all soil depths and topographic positions was greatest when soils were dry and decreased under wet soil conditions; this variability remained high in the deeper soil horizons, regardless of season. Lastly, event analysis suggests that the response to early season rainfall was highly variable along the hillslopes and was likely dominated by localized controls such as microtopography and vegetation as well as soil texture, antecedent moisture conditions, and rainfall characteristics. Our results suggest that the drivers of wet and dry season soil moisture dynamics can vary across topographic positions along a hillslope and do not always follow topographic controls.

Plain Language Summary In Mediterranean climates, the amount of water stored in a soil is extremely important for plant transpiration and growth during the dry season and for streamflow generation during the wet season. During wet periods, the patterns of wet and dry soil across a hillslope generally correlate to topography and precipitation magnitude and frequency, with soils nearest the stream staying wetter and soils furthest from the stream staying drier. In contrast, during dry periods, soil wetness across the landscape is generally variable and largely determined by how much water the plants are using in a particular location. This study looked at the patterns of soil moisture across a hillslope over wet and dry periods to explore the dominant controls on soil moisture. We found that sites nearest the stream generally stayed wet during the wet and dry seasons, but that ridgetops located far from the stream channel were consistently wetter than mid-slope positions during the rainy season. We also found little difference in soil moisture within the rooting zone among topographic positions. The transition from wet to dry conditions was highly variable among hillslope positions and depths and this likely reflected unmeasured factors such as small differences in local topography and vegetation.

1. Introduction

Soil water storage exerts a dominant control over hydrological exports of streamflow and evapotranspiration from a catchment. In Mediterranean climates, the soil storage capacity in a catchment is especially critical, as winter precipitation inputs are out of phase with summer plant water use (Baldocchi & Xu, 2007; Link et al., 2014). For forested landscapes in these climates, the trees are dependent on the reserve of water that exists both in the soils and subsurface saprolite and bedrock at the end of the wet season to sustain ecohydrological functions during the dry months (e.g., Hahm et al., 2019; Klos et al., 2018). Comparatively, during the rainy season, soil water storage represents an important control over the timing and magnitude of stormflow events (Western & Grayson, 1998; Zehe et al., 2010), with important implications for aquatic ecosystems and downstream communities and infrastructure. The balance between catchment water inputs and water exports in Mediterranean climates is becoming increasingly uncertain with greater water deficits, as global temperatures have warmed, atmospheric vapor pressure deficits have increased, and periods of drought have lengthened (Eamus et al., 2013; Goulden & Bales, 2019; Yuan et al., 2019). Thus, improved understanding of how soils store and release water over wet and dry seasons is critical for predicting the resilience of forest ecosystems to fluctuations in climate as well as for managing forest and water resources (Tague et al., 2019).

Soil water content is often heterogeneous in both space and time across hillslopes and catchments, which has hindered our ability to model and predict soil water storage and release (Famiglietti et al., 1998; Rodriguez-Iturbe et al., 1999; Schmugge & Jackson, 1996; Western et al., 1999). Variability in soil water is most evident in montane catchments in part due to high heterogeneity in soil properties and steep topography (Teuling & Troch, 2005). For example, the variability in soil water content has been related to a broad range of soil physical properties, including soil texture (e.g., Saxton et al., 1986; Warren et al., 2005), bulk density (Cosh et al., 2008), soil depth (e.g., Liang & Chan, 2017; Tromp-van Meerveld & McDonnell, 2006), and the amount and density of rock content (Naseri et al., 2019). Soil water content has also been shown to vary with vegetation rooting depth, rooting density, and evapotranspiration rates (e.g., Bréda et al., 1995; Klein et al., 2014; Tromp-van Meerveld & McDonnell, 2006). The dominant controls over the spatial patterns in soil moisture have been observed to shift seasonally as the mean soil moisture state transitions from "wet" to "dry" (Bell et al., 1980; Famiglietti et al., 1999, 1998, 2008; Hills & Reynolds, 1969; Western & Blöschl, 1999). For example, Grayson et al. (1997) and Western et al. (1999) found a high degree of spatial organization during the wet state, which they attributed to strong topographic influence (i.e., nonlocal controls). Alternatively, during the dry state, the dominant controls switched such that the spatial variability in soil water content was driven by site-specific soil properties (i.e., local controls) (Grayson et al., 1997; Western et al., 1999).

In contrast to these previous studies, some have shown that soil moisture variability is greatest when moisture is closest to its mean, as some soils may dry due to rapid drainage while other soils might remain wet due to disconnected soil pathways or impeding soil layers (Hills & Reynolds, 1969). The soil moisture status during wetting periods related to rainfall or snowmelt events and the drying periods that follow may therefore have strong controls on runoff mechanisms, and it follows that the ability to predict the moisture state could lead to improvements in forecasting the amount and timing of runoff. Alternatively, multiple grassland studies have posited that soil moisture heterogeneity will reach a maximum following rain events due to differences in infiltration rates, while heterogeneity may be at a minimum during dry periods when soils have drained relatively uniformly to a low moisture state (Famiglietti et al., 1998; Reynolds, 1970). Understanding the variability in soil moisture during both wet and dry seasons across diverse ecosystems is especially important for predicting ecosystem resilience to droughts and climate change, as departures from historical variability may lead to decreased ecohydrological function of the catchment (Aulenbach & Peters, 2018; Oishi et al., 2010; Orth & Seneviratne, 2013).

Previous studies have attempted to understand the variability in soil moisture across seasons, hillslopes, and soil depths (e.g., Famiglietti et al., 1998; Penna et al., 2013; Tromp-van Meerveld & McDonnell, 2006). Spatially, soil moisture often varies according to local topographic controls, which can dictate both soil depth and depth to groundwater—Soils are generally wettest at the bottom of a hillslope and driest at the top (Beven & Kirkby, 1979; Burt & Butcher, 1985; Famiglietti et al., 1998). Furthermore, soil moisture can vary with hillslope shape, as slopes with either planar or profile concave curvature often accumulate water and generate subsurface runoff to a greater degree than convex hillslopes (Anderson & Burt, 1978; Moore et al., 1988; Nyberg, 1996). Additional variation in soil moisture can be caused by slope angle with gentler slopes generally displaying greater wetness due to higher infiltration rates, deeper soils, shallower depth to groundwater, lower subsurface drainage rates, and lower overland flow (Hills & Reynolds, 1969; Moore et al., 1988; Nyberg, 1996)

While soil moisture generally increases with increasing soil depth, it may also be highly variable vertically through the soil profile (Brooks et al., 2010; Sprenger et al., 2019). Such vertical and lateral variations in soil moisture are controlled in part by the heterogeneity of soil characteristics, distribution of vegetation, and hydrologic routing across a catchment (Beven & Kirkby, 1979; Daly et al., 2004a, 2004b; Dunne & Black, 1970; T. Dunne et al., 1975; Dymond et al., 2017; Price & Bauer, 1984; Tromp-van Meerveld & Mc-

10.1029/2020WR029170

Donnell, 2006). Additional variation in soil moisture is driven by characteristics of precipitation inputs (e.g., precipitation or snowmelt intensity, overall depth, and event duration) and the vertical and horizontal movement of wetting fronts as water infiltrates into the soil profile. The influence of the aforementioned characteristics on catchment soil moisture dynamics are further controlled by local climate and antecedent soil moisture conditions (Allan & Roulet, 1994; Black, 1972; Famiglietti et al., 1998; Lawrence & Hornberger, 2007). Because catchment soil moisture exerts a critical control over both streamflow generation (Anderson & Burt, 1978; Dunne & Black, 1970; Dunne et al., 1975) and transpiration (Breshears et al., 2009; Daly et al., 2004a, 2004b; Tromp-van Meerveld & McDonnell, 2006), understanding soil moisture dynamics across space and time is essential to understanding the integrated ecohydrological behavior of a catchment.

While process-based hydrologic models have integrated the shifting spatial and temporal patterns in subsurface water storage and movement (e.g., Band, 1986; Ivanov et al., 2008a, 2008b; Tague & Band, 2004; Vertessy et al., 1993; Wigmosta et al., 1994), quantifying and investigating soil moisture dynamics across hillslopes and seasons remain a key component to understanding water storage and release in a catchment. Thus, our research goal was to characterize the distribution and patterns of soil moisture across hillslopes to identify the hydrologic processes that lead to converging or diverging moisture states across vertical soil profiles. We used a well-studied Mediterranean climate research site, the Caspar Creek Experimental Watersheds, to address the following objectives:

1. Quantify the temporal and spatial variability around mean moisture states in vertical soil profiles across a topographic gradient
2. Explore how soil water content varied across hillslope positions in response to rainfall events during early, mid, and late-season storms; and
3. Quantify the differences in drawdown of soil water across hillslope positions and the vertical soil profile as soils transitioned from wet to dry

We hypothesized that the soil moisture content across topographic gradients and soil profiles (i.e., soil depths) would be the least variable during the wet season, with positions lower on the hillslope and deeper in the soil profile exhibiting higher overall soil moisture contents than topographically distant positions and shallow soil depths. We also hypothesized that during the dry season, soil moisture would be most variable across all topographic positions and depths due to the depletion of soil water by evapotranspiration.

2. Study Site

Our study site was in the coast redwood forest fog belt in northern California, which is increasingly threatened due to warming summertime temperatures (Pierce et al., 2018), decreasing fog (Johnstone & Dawson, 2010), and increasing threats from wildfire (Westerling & Bryant, 2007). The Caspar Creek Experimental Watersheds (39°21′N, 123°44′W) are located on the Jackson Demonstration State Forest (JDSF) in northwestern California (Figure 1), approximately 7 km from the Pacific Ocean (Henry, 1998). Established as a cooperative study between the USDA Forest Service and the California Department of Forestry and Fire Protection in 1961, research at Caspar Creek has focused on streamflow and sediment production in a coast redwood forest (e.g., Keppeler & Ziemer, 1990; Lisle, 1989; Reid et al., 2010). While the broad study area includes two principal watersheds, our study focused on the South Fork Caspar Creek watershed, which has a drainage area of 417 ha. Specifically, our study focused on three sub-watersheds within the South Fork: Treat, Williams, and Ziemer (Figure 1).

The climate at Caspar Creek is Mediterranean (Köppen-Geiger Csb), with cool, dry summers characterized by coastal fog and mild, moist winters. The 30-year mean annual precipitation measured near the confluence of the South Fork and North Fork from 1989–2018 was 1,168 mm, with 93% of the rainfall occurring from October to April. Snowfall is rare in the watershed. The mean monthly temperature measured near the South Fork weir from 1989–2018 averaged 6.1°C in December and 13.7°C in August. The elevations in the three sub-watersheds range from 70 to 320 m and average hillslope gradients from the channel to ridge vary from 15° to 35° (27%–70%). Soils in the South Fork range from approximately 100 to 300 cm in depth (Table 1) and are predominately well-drained clay-loam Ultisols and Alfisols derived from Franciscan sandstones and shales (Rittiman & Thorson, 2006). Discontinuous argillic horizons occur within the soil profile and hand-auguring efforts reached saprolite at depths that ranged from 107 to 282 cm, and the

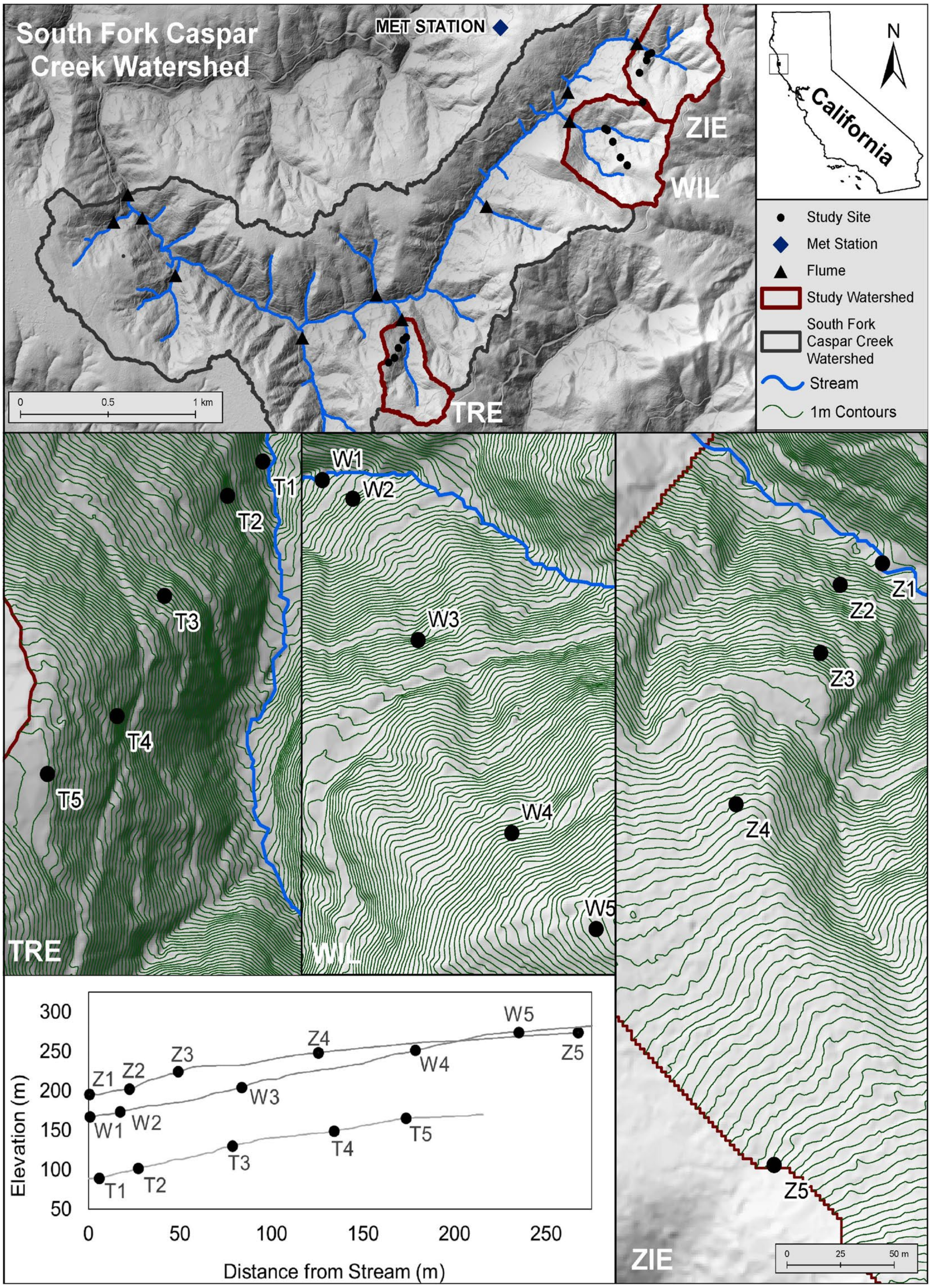

Figure 1. The South Fork Caspar Creek is located on the coast of northern California (inset). There are 10 gauged sub-watersheds that drain to the South Fork weir. We included hillslope transects along the Treat, Williams, and Ziemer sub-watersheds in our analysis. Hillslope profiles in the lower inset graphic show the elevation of each site along the transect position.

Table 1
Study Locations Included Five Topographic Positions Replicated Across Three Sub-Watersheds in the South Fork Caspar Creek

Sub-watershed name	ID	Topographic position	Soil depth (cm)[a]	Boring depth (cm)[b]	Slope (%)	Aspect (°)	Elevation (m)	Mean canopy closure (%)
Treat	TRE	1-Riparian	111	150	60	86	89.0	93.6
		2-Toeslope	282	550	55	77	101.2	93.8
		3-Sideslope	222	500	45	38	130.2	90.9
		4-Shoulder	145	608	70	105	148.7	91.2
		5-Ridge	254	682	36	91	165.1	93.3
Williams	WIL	1- Riparian	221	432	46	300	166.4	95.6
		2-Toeslope	193	363	50	320	173.1	93.9
		3-Sideslope	107	183	80	350	203.9	93.7
		4-Shoulder	152	754	55	357	251.5	90.1
		5-Ridge	155	760	25	288	274.0	94.0
Ziemer	ZIE	1- Riparian	107	158	15	10	196.2	93.1
		2-Toeslope	234	292	55	0	201.9	89.9
		3-Sideslope	184	258	85	18	224.1	90.2
		4-Shoulder	136	429	28	351	248.0	89.4
		5-Ridge	196	406	19	294	270.4	89.9

Note. Slope and aspect represent the local conditions.
[a]Depth to soil-saprolite boundary. [b]Approximate depth to unweathered bedrock.

variable saprolite layer extended to depths of up to 760 cm (Table 1). We considered saprolite to consist of chemically weathered bedrock, which often forms in regions with high rainfall. Given that boreholes were hand-augured, the depth to bedrock should be taken as approximate depths. The underlying geology across Caspar Creek consists of the Coastal Belt of the Franciscan Complex; the Franciscan coastal belt assemblage contains deformed sedimentary bedrocks of varying degrees, while the assemblage in Caspar Creek consists of softer mudstone, claystones, and shales when compared to terrains that contain harder and less deformed graywackes and cherts (Spittler, 1995).

Rainfall is routed to stream channels primarily via subsurface flow, including preferential flow paths in both the soil and saprolite except in areas where soils have been compacted or otherwise disturbed. In particular, soil pipes are an important hillslope drainage mechanism (Keppeler & Brown, 1998). Vegetation in the South Fork is dominated by third-growth coast redwood (*Sequoia sempervirens* (D. Don) Endl.), Douglas-fir (*Pseudotsuga menziesii* (Mirb.) Franco), grand fir (*Abies grandis* (Doug. ex D. Don) Lindl.), and western hemlock (*Tsuga heterophylla* (Raf.) Sarg.), with smaller amounts of tanoak (*Lithocarpus densiflorus* (Fook. and Arn.) Rohn) and red alder (*Alnus rubus* Bong.). The old-growth coast redwood in Caspar Creek, similar to the majority of the region, was clear-cut in the late nineteenth and early twentieth centuries; a selection harvest in the South Fork, including the three study sub-watersheds, removed 63% of the second-growth forest from 1971 to 1973. It is important to note that the presence of large roots and the legacy effects of logging likely influence the spatial variability of moisture dynamics in this region.

3. Methods

3.1. General Study Design and Field Methods

In summer 2015, we instrumented hillslope transects in three sub-watersheds in the South Fork catchment (Figure 1), which had similar elevations, slopes, and dominant soil types. All transects were roughly north-facing and included five topographic positions: riparian, toeslope, sideslope, shoulder, and ridge (Figure 1). Topographic positions were selected in the field and named following terminology of Ruhe and Walker (1968) and Miller and Schaetzl (2015), with some slight modifications (see Table S1 in the Supporting Information S1). Local aspect and slope were measured across a 25- m profile using a compass and clinometer, while canopy closure data were collected in September 2017 using hemispherical photos. Hemispherical photos were taken with a digital single-lens reflex camera (Nikon P5000 or D7100; Nikon Corporation) with a circular fisheye lens (Nikon FC-E8, Nikon Corporation, Tokyo, Japan; or Sigma 4.5 mm, f/2.8 EX DC HSM) at 1 m above the ground and percent tree canopy closure was calculated using the HemiView Software (Delta-T Devices Ltd) (Table 1).

To quantify soil water content, we installed METER EC5 sensors (METER Group, Inc.; resolution: 0.001 m^3 m^{-3}; accuracy ± 0.03 m^3 m^{-3}) vertically into the soil at 15, 30, and 100 cm depths. Sensors were installed at all five topographic positions in each of the study sub-watersheds (15 sample sites, 45 total sensors) and connected to EM60 data loggers, which recorded data every 10 minutes (Onset Computer Corp.). Data for each sensor were averaged to determine hourly or daily volumetric water content (cm^3 cm^{-3}) for each water year (WY; October 1 of the previous year to September 30 of the current year). Our study consisted of two full years of data (WY16 and WY17), as the study sites were harvested in the middle of WY18 for a related experiment (Dymond et al., 2021).

We used the augured holes to describe the soil profiles (Table S2 in the Supporting Information S1) and collected samples to determine soil texture. Samples were dried at 105°C for 24 hr, mechanically disaggregated using a ceramic mortar and rubber-tipped pestle and dry-sieved using a 2 mm sieve. A 1–2 g subsample of the <2 mm fraction and a gravimetrically proportionate subsample of the >2 mm fraction were then combined and wet-sieved with a 2 mm sieve. Two drops of Beckman IIA anionic dispersant were added to the fine fraction of the subsample, which was then sonicated at power setting four for three minutes before the volumetric particle size distribution was determined using a Beckman Coulter LS13320 particle size analyzer (Beckman Coulter, Brea). Core samples (250 mL each) were obtained from a subsample of locations selected to represent different soil textures and hillslope positions (T1 15, 30, 100; T3 15, 30, 100; W1 15; W2 15; W3 15; W4 15, 30, 100; W5 15; Z2 15; Z4 15; and Z5 15) in October 2019. We used the core samples to quantify the relationship between volumetric water content and matric potentials across a range of tensions from saturation to 3 pF (−0.1 MPa) using a HYROP instrument (METER Group Inc.). We also used the cores to quantify soil bulk density, porosity, and saturated hydraulic conductivity. We used five 2–3 g subsamples from each core to determine water release characteristics for tensions between 4 pF (−1 MPa) and 6.5 pF (−320 MPa) using a WP4C instrument (METER Group Inc.). Soil moisture release curves were fit across the range of measurements by selecting the variation of the van Genuchten model that visually appeared to best fit the data using the HYPPROP-FIT software (van Genuchten, 1980) (METER Group Inc.). Moisture contents at wilting point (4.2 pF or −1.5 MPa) and field capacity (1.8 pF or −6.2 kPa) were determined from the fitted data.

As soil texture did not vary much among the sub-watersheds, we considered the observations from each topographic position and soil depth in the three study sub-watersheds to be replicates ($n = 3$ for each topographic position and soil depth combination; Table 2). There was no significant difference in percent sand, silt, and clay fraction across similar soil depths and topographic positions ($\alpha = 0.05$). While there were likely slight differences in other edaphic characteristics (e.g., organic matter content, rooting depth, etc.) across the replicates, we assumed that these potential differences were negligible and the uncertainty that they may have contributed to the soil moisture responses was less than the precision of the soil moisture sensors.

3.2. Wet and Dry Season Soil Moisture Characteristics

We first investigated relative wetness across topographic positions and soil depths. The goal of this analysis was to explore temporal and spatial variability around seasonal moisture states to see if hillslopes and vertical soil profiles converged around a mean soil moisture or if daily soil moisture was highly variable. To accomplish this goal, daily volumetric water content (VWC) at each topographic position and depth ($n = 3$ replicates per topographic position/depth) was first characterized using the mean ($\bar{x}$) and standard deviation (s) across wet and dry seasons for WY16 and WY17. Seasonality was based on whether precipitation inputs (total monthly precipitation) exceeded Thornthwaite potential evapotranspiration (PET; Thornthwaite, 1948) or vice versa. Season was defined to remove the variability associated with transitional moisture states. Thus, we considered the wet season to include December to March and the dry season to include June to September. Differences between mean VWC for the wet and dry seasons across topographic posi-

Table 2
Soil Texture, Mean Percent Clay, Silt, and Sand, Field Capacity (FC), Wilting Point (WP), and Saturated Hydraulic Conductivity (k_{sat}) for Three Soil Depths and Five Topographic Positions as Averaged Across Three Study Sub-Watersheds in the South Fork, Caspar Creek

Topographic position	Soil depth (cm)	Soil texture	% Clay fraction	% Silt fraction	% Sand fraction	FC (cm^3 cm^{-3})	WP (cm^3 cm^{-3})	k_{sat} ($cm\ s^{-1}$)
Riparian	15	Sandy loam	4.3 (2.5)	32 (11)	63 (13)	0.22 (0.1)	0.13 (0.0)	7.2E−02
	30[a]	Sandy loam	3.3 (2.6)	25 (12)	72 (15)	0.23 (0.0)	0.15 (0.0)	3.8E−02
	100[a]	Sandy loam	3.3 (0.2)	28 (3.8)	69 (3.9)	0.27 (0.0)	0.17 (0.0)	2.8E−02
Toeslope	15	Sandy loam	3.6 (0.7)	31 (6.2)	66 (6.8)	0.19 (0.0)	0.13 (0.0)	1.5E−02
	30[a]	Sandy loam	4.1 (1.6)	29 (11)	66 (12)	0.19 (0.0)	0.13 (0.0)	1.6E−02
	100[a]	Sandy loam	4.8 (1.4)	38 (16)	57 (18)	0.22 (0.0)	0.13 (0.0)	4.4E−03
Sideslope	15	Sandy loam	4.4 (1.1)	38 (16)	57 (18)	0.21 (0.0)	0.14 (0.0)	1.8E−02
	30	Sandy loam	5.6 (1.2)	41 (7.8)	53 (8.9)	0.21 (0.0)	0.13 (0.0)	1.8E−02
	100	Sandy loam	5.8 (1.0)	39 (2.3)	55 (3.1)	0.22 (0.0)	0.15 (0.0)	2.9E−02
Shoulder	15	Sandy loam	4.4 (1.2)	36 (11)	60 (12)	0.22 (0.0)	0.13 (0.0)	2.0E−02
	30	Loam	7.8 (1.8)	46 (7.4)	46 (9.0)	0.23 (0.0)	0.13 (0.0)	7.1E−03
	100	Sandy loam	5.5 (2.7)	36 (11)	59 (13)	0.24 (0.0)	0.14 (0.0)	3.8E−03
Ridge	15	Sandy loam	5.5 (1.5)	36 (5.9)	59 (4.7)	0.21 (0.0)	0.11 (0.0)	7.0E−03
	30	Sandy loam	4.6 (1.1)	35 (4.2)	60 (5.3)	0.20 (0.0)	0.13 (0.0)	2.0E−02
	100	Sandy loam	5.9 (2.4)	38 (9.9)	56 (12)	0.22 (0.0)	0.13 (0.0)	2.1E−02

Note. Standard deviations are shown in parentheses.
[a]All samples were collected at soil moisture sensor locations except W1-30, W1-100, W2-30, and W2-100 which were from corresponding depths in the piezometer cores.

tions and soil depths were determined using Tukey's honestly significant differences (HSD) with $\alpha = 0.05$ in R version 4.0.2 (R Core Development Team, 2020).

We then determined the probability density function of daily soil moisture during the wet and dry seasons from each depth and topographic position using kernel density estimation scaled for sample size using the *ggridges* package (Wilke, 2020) in R version 4.0.2 (R Core Development Team, 2020). This analysis was used to detect patterns in daily soil moisture across the wet and dry seasons that might not be immediately evident in traditional summary statistics.

3.3. Event Analysis

We measured precipitation with an unshielded OTT Pluvio N all-weather weighing rain gauge (OTT HydroMet; 0.025 mm resolution), which was installed at a height of 1.5 m at the meteorological station on the north ridge of the South Fork catchment (Figure 1). Precipitation was recorded at 15 min intervals using a CR1000 data logger (Campbell Scientific Inc.). An individual precipitation event was determined if there was an accumulation of at least 5 mm of precipitation and was separated by a period of at least six hours with less than 5 mm of precipitation. We assumed precipitation was generally constant (varied by less than 5%) across the sub-watersheds, as lapse rates due to orographic effects were likely minor across the sub-watersheds. Total precipitation was above normal (116 cm) for both study years, with WY17 (182 cm) receiving 37 cm more rainfall than WY16 (145 cm) (Figure 2).

We investigated the vertical soil moisture responses across the hillslopes following three precipitation events in both WY16 and WY17 ($n = 6$ events; Table S3 in the Supporting Information S1). First, we identified the first event with greater than 2.5 cm of rain over a 24- hr period to better understand how the different soil depths and topographic positions transitioned from dry antecedent moisture conditions to wetter conditions after the initial onset of precipitation. Next, we identified the largest event in each water year, regardless of the timing. Lastly, we looked at the last event with at least 2.5 cm precipitation in a 24- hr

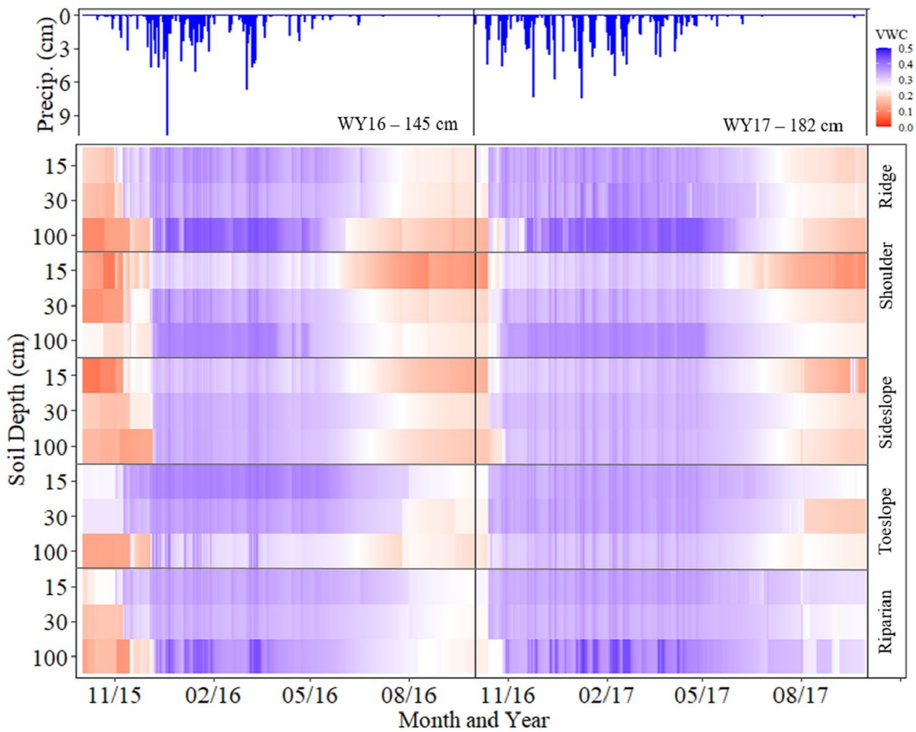

Figure 2. Daily precipitation and corresponding daily volumetric water content (VWC; cm^3 cm^{-3}) across water years 2016 and 2017 for three soil depths (15, 30, and 100 cm) and five topographic positions. VWC data are means across the three sub-watersheds. Vertical bar represents the break between water years.

period. For the event analysis, we averaged the data across the three study sub-watershed sites to obtain one value per soil depth and topographic position for each 10-min interval.

Responses to precipitation inputs were analyzed using multiple metrics. First, we looked at the change in volumetric soil moisture (cm^3 cm^{-3}) from the antecedent conditions, calculated as the difference between the 10-min soil moisture prior to the onset of precipitation and maximum soil moisture within six hours of rainfall cessation. We chose a period of six hours following rainfall cessation based on visual estimates of how quickly soil moisture responded to an influx of precipitation and to ensure that calculations were not influenced by additional rainfall from new precipitation events. Second, we quantified the response time of the soil to the start of the precipitation event (lag time), which was the time for soil moisture to increase by at least 0.5% (0.005 cm^3 cm^{-3}) from the previous value. Lastly, we quantified lag to peak or the time between the initial soil moisture response and the maximum soil moisture for the event. We focused our efforts on quantifying the rising limb of the soil moisture hydrograph, as the recession of soil moisture was often affected by subsequent events. All event analyses were conducted using a 60- min timestep to account for possible differences in the onset of precipitation and soil moisture responses across the watersheds. All event response metrics represent one value per each of the three soil moisture depths across the five topographic positions.

3.4. Quantifying Soil Water Drawdown

Our last objective was to investigate the transition of soils from wet to dry conditions across the different topographic positions and soil depths using the timing and rate of the soil drawdown. The date of the last rainfall event that exceeded 5 mm day^{-1} was used as the start of the drawdown period, which was May 6 in WY2016 and April 27 in WY2017. Meteorological conditions were chosen to start the drawdown period instead of soil moisture conditions or a set calendar date to (a) homogenize the start of the drawdown periods across the topographic positions and soil depths, and (b) better capture the timing of the drawdown across the study years. The end of the soil drawdown period was defined as the minimum soil moisture value prior to the onset of the next rainy season. For both water years, the minimum occurred in the next water year. Lastly, we fit an exponential decay curve to the drawdown period to compare the rate of soil drawdown across topographic positions and soil depths during the two study years.

4. Results

4.1. Temporal Soil Moisture Dynamics

Across the two years, there were clear transitions between periods of soil wetting during the rainy seasons and periods of soil drying during the ET-dominated seasons (Figure 2). In WY16, the transition from dry to wet soils occurred first in the shallowest soil depths and later in the deeper soils. However, in WY17, soils transitioned from dry to wet more uniformly across the soil depths at all topographic hillslope positions.

During the wet winter months, precipitation appeared to percolate rapidly through the soil profile, resulting in increased soil water content in the deeper soil layers relative to the shallow soil layers (Figure 2). This rapid percolation was still at a coarse temporal resolution (i.e., one day) and can be seen in the vertical blue striping pattern during the wet season in Figure 2. In contrast to the quick wet-up of soils during the rainy season, the transition to the dry season progressed more slowly across all soil depths and topographic positions, which was apparent in the smoother color transitions in the second half of each water year in Figure 2.

Ridges maintained high soil moisture contents during the wet season, particularly deeper in the soil profile (Figure 2). Soil moisture at 100 cm in the ridges was consistently greater than 0.4 during both WY16 and WY17—this was constant across the three study sub-watersheds and not driven by any one particular site. Sideslope and shoulder positions generally dried earlier and the dryness persisted longer during the summer months than it did at the riparian, toeslope, and ridge positions. When aggregated across water years and soil depths, Tukey HSD tests revealed that mean daily soil moisture across the topographic positions were all different from one another except for the sideslope and shoulder positions.

When aggregated into mean monthly soil moisture, there were also clear transitions between wet and dry soil moisture states across the topographic positions and soil depths (Figure 3). Mean monthly soil moisture was at a minimum in the early fall and reached its maximum in mid-winter, regardless of soil depth or topographic position. The period of soil drying was consistent with ET-dominated conditions, approximately May through September. At the monthly scale, the relationships between topography and soil depth were more apparent than at the daily timestep. At 15 cm, riparian, toeslope, and ridge positions were wettest during the wet season. During the dry season, ridges transitioned into being the driest location on the hillslope. At 30 cm depth, there were no apparent differences in soil moisture among the topographic positions. Additionally, the magnitude of change between the wettest and the driest soils at the 30 cm depth was smaller than the range from the other soil depths. Lastly, at 100 cm, soil moisture was highly variable with no apparent patterns across topographic positions (Figure 3).

4.2. Wet and Dry Season Soil Moisture

During the wet season, positions lower on the hillslope and deeper in the soil profile were wetter overall (Table 3). While the shallow depths (15 cm) in the riparian and toeslope positions were wetter than the corresponding depth at the steeper sideslope and shoulder positions during the wet season, the ridges remained the wettest positions on the hillslope, regardless of soil depth (Table 3). At 30 cm soil depth, there was no discernable difference in mean wet season soil moisture content across the topographic positions.

During the dry season, the ridges changed from being the wettest on the hillslope to being one of the driest topographic positions. This was particularly true deeper in the soil profile and is emphasized by its greater amplitude ($\bar{A}$; Table 3). In general, the deeper soil depths displayed the largest differences between minimum and maximum daily VWC (Table 3). The shallow soils at the sideslope and shoulders were significantly drier than the other topographic positions.

10.1029/2020WR029170

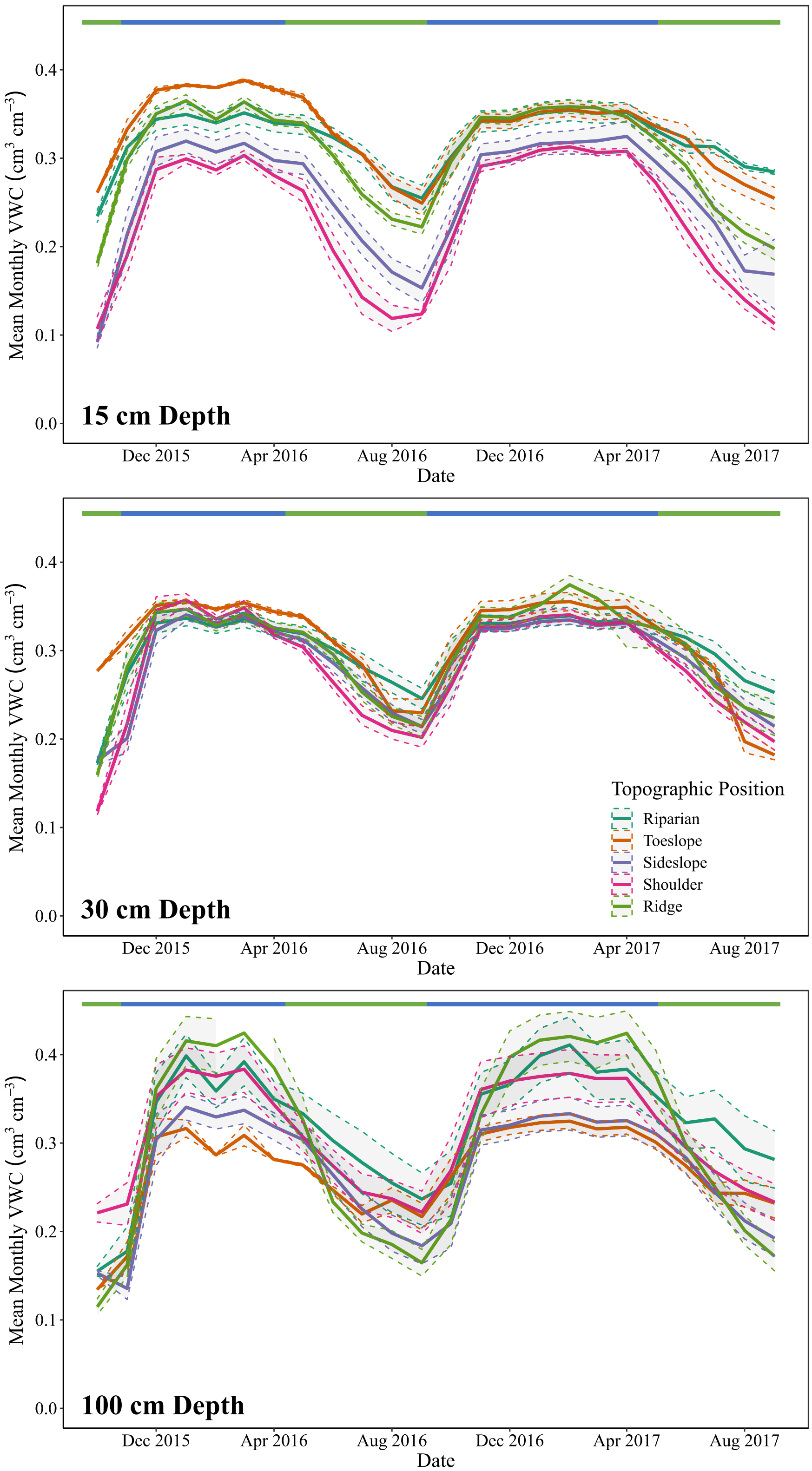

Figure 3. Mean monthly volumetric water content ($cm^3\ cm^{-3}$) at 15 cm (top), 30 cm (middle), and 100 cm (bottom) of the soil profile for five topographic positions as measured from WY16 through WY17. Shaded regions within dashed bands represent 95% confidence intervals. Blue bars represent periods when P > PET, while green bars represent periods when PET < P.

10.1029/2020WR029170

Table 3
Wet Season (December–March) and Dry Season (June–September) Mean Daily Volumetric Soil Moisture Across Three Study Sub-Watersheds and Two Years, Mean Minimum Daily Volumetric Soil Moisture, and the Mean Range in Daily Volumetric Water Content (Amplitude; $\bar{A}_{vwc}$)

Topographic position	Soil depth (cm)	Wet season $\bar{x}_{vwc}$ (s_{vwc})	Dry season $\bar{x}_{vwc}$ (s_{vwc})	Minimum $\bar{x}_{vwc}$ (s_{vwc})	$\bar{A}_{vwc}$ (s_{vwc})
Riparian	15	0.34 (0.03)	0.29 (0.04)	0.23 (0.03)	0.14 (0.05)
	30	0.33 (0.03)	0.28 (0.04)	0.20 (0.05)	0.17 (0.05)
	100	0.37 (0.08)	0.28 (0.10)	0.17 (0.09)	0.29 (0.09)
Toeslope	15	0.35 (0.03)	0.28 (0.05)	0.24 (0.04)	0.11 (0.05)
	30	0.34 (0.03)	0.25 (0.05)	0.19 (0.04)	0.14 (0.08)
	100	0.32 (0.03)	0.24 (0.04)	0.20 (0.05)	0.15 (0.10)
Sideslope	15	0.31 (0.04)	0.21 (0.07)	0.13 (0.05)	0.14 (0.02)
	30	0.33 (0.02)	0.25 (0.04)	0.18 (0.03)	0.17 (0.03)
	100	0.34 (0.05)	0.24 (0.07)	0.15 (0.06)	0.29 (0.03)
Shoulder	15	0.30 (0.02)	0.16 (0.05)	0.09 (0.03)	0.23 (0.03)
	30	0.34 (0.03)	0.24 (0.05)	0.17 (0.05)	0.22 (0.08)
	100	0.36 (0.08)	0.27 (0.06)	0.20 (0.06)	0.19 (0.07)
Ridge	15	0.35 (0.02)	0.25 (0.04)	0.19 (0.04)	0.20 (0.03)
	30	0.35 (0.03)	0.26 (0.05)	0.18 (0.04)	0.22 (0.05)
	100	0.38 (0.09)	0.22 (0.06)	0.14 (0.04)	0.30 (0.04)

Note. Standard deviations are shown in parentheses. Data are shown by topographic position and soil depth.

Tukey's HSD tests revealed nuances in the differences between wet and dry season soil moisture across both the topographic positions and soil depths. We found that there were more significant differences in soil moisture among topographic positions during the wet season (Figure 4). During the dry season, the positions lower on the hillslope generally had greater moisture contents than the positions higher on the hillslope, with the exception of 30 cm depth, where soil moisture was the same regardless of topographic position (Figures 3 and 4). During the wet season, however, the patterns of soil moisture across the hillslope generally did not follow typical conventions of wetter soils downslope due to interflow or overland flow. At shallow soil depths, the low and high topographic positions were the wettest, but at deeper soil depths, the riparian, shoulder, and ridge sites were the wettest (Figure 4).

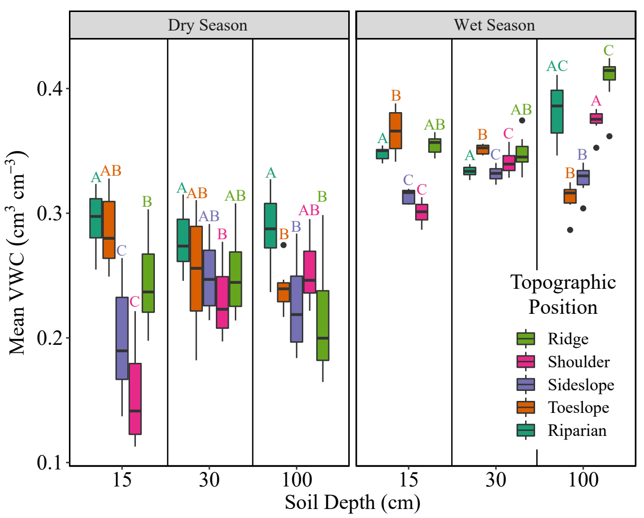

Figure 4. Boxplots of mean daily soil moisture (cm³ cm⁻³) for five topographic positions and three soil depths for dry seasons (May–September) and wet seasons (October–April). A, B, and C denote significant differences in wet and dry season mean volumetric water content between topographic positions at soil depths of 15, 30, and 100 cm. Differences were determined by Tukey's honestly significant differences ($\alpha = 0.05$).

Ridgeline plots help to illustrate the complexity of organization into wet and dry moisture states across the topographic positions and soil depths (Figure 5). During the wet season (December through March), we expected to see a relatively unimodal distribution of soil moisture around the mean. While this was true for some topographic positions and soil depths, it was not universal (Figure 5). The shallow riparian sites approached a bimodal distribution, while the shallow sideslope sites lacked any apparent distribution. The deeper soil moisture (100 cm) had large ranges across all topographic positions, with no evidence of mean moisture states.

In contrast, soils during the dry season had distributions that were wider, with dampened peaks compared to the wet season (Figure 5). Some sites, particularly topographic positions that were lower on the hillslope, approached bi-modal distributions. While the deeper soils generally had

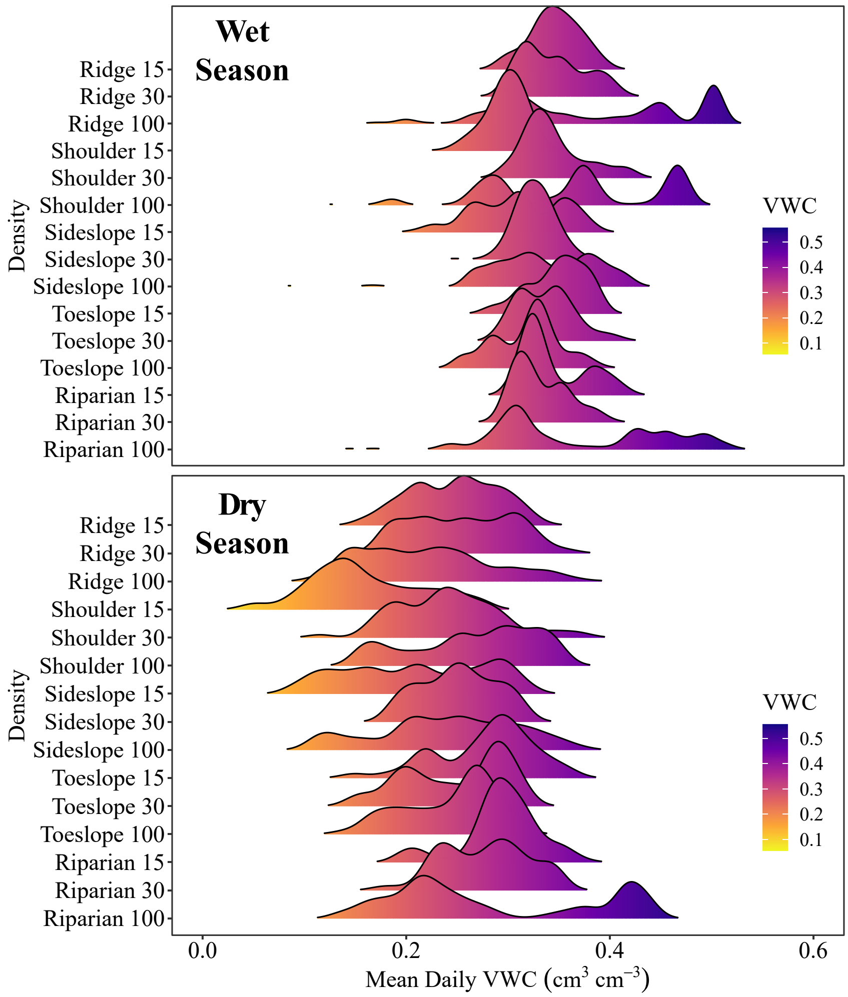

Figure 5. Ridgeline plots of mean daily volumetric water content ($cm^3\ cm^{-3}$) by topographic position for three soil depths for wet (December–March) and dry (June–September) seasons.

greater variability in soil moisture than the shallower soil depths in the dry season, the variability during the dry season was less than that of the same locations during the wet season (Figure 5).

4.3. Wet Season Event Analysis

We used the first large precipitation event (24 hr precipitation of at least 2.5 cm) of each year to investigate patterns in spatial and vertical soil moisture. In the drier WY16, the hillslope quickly responded to the first event (November 14, 2015) and reached maximum soil moisture either prior to or within two hours of the event cessation (Figure 6). There were a few exceptions to this, most noticeably at the sideslopes, where both the 30 and 100 cm depths had delayed lag times and lag to peak times that exceeded one day following rainfall cessation. At both depths, there was only a slight increase in soil moisture during and following the event. The percent change in soil moisture from the start to the end of the event at the deep sideslopes was only 0.03%.

In contrast, the lag times for the first event of WY17 (October 13, 2016) were longer (Figure 6). Notably, the first event in WY16 was 30 days earlier than the first event in WY17. WY16 was also the end of one of the most severe droughts on record in the region (Robeson, 2015). The uniform wetting of the soils in all but some of the sideslope positions was less apparent in WY17 and there was no distinct pattern in responses to the precipitation across soil depths or topographic positions.

10.1029/2020WR029170

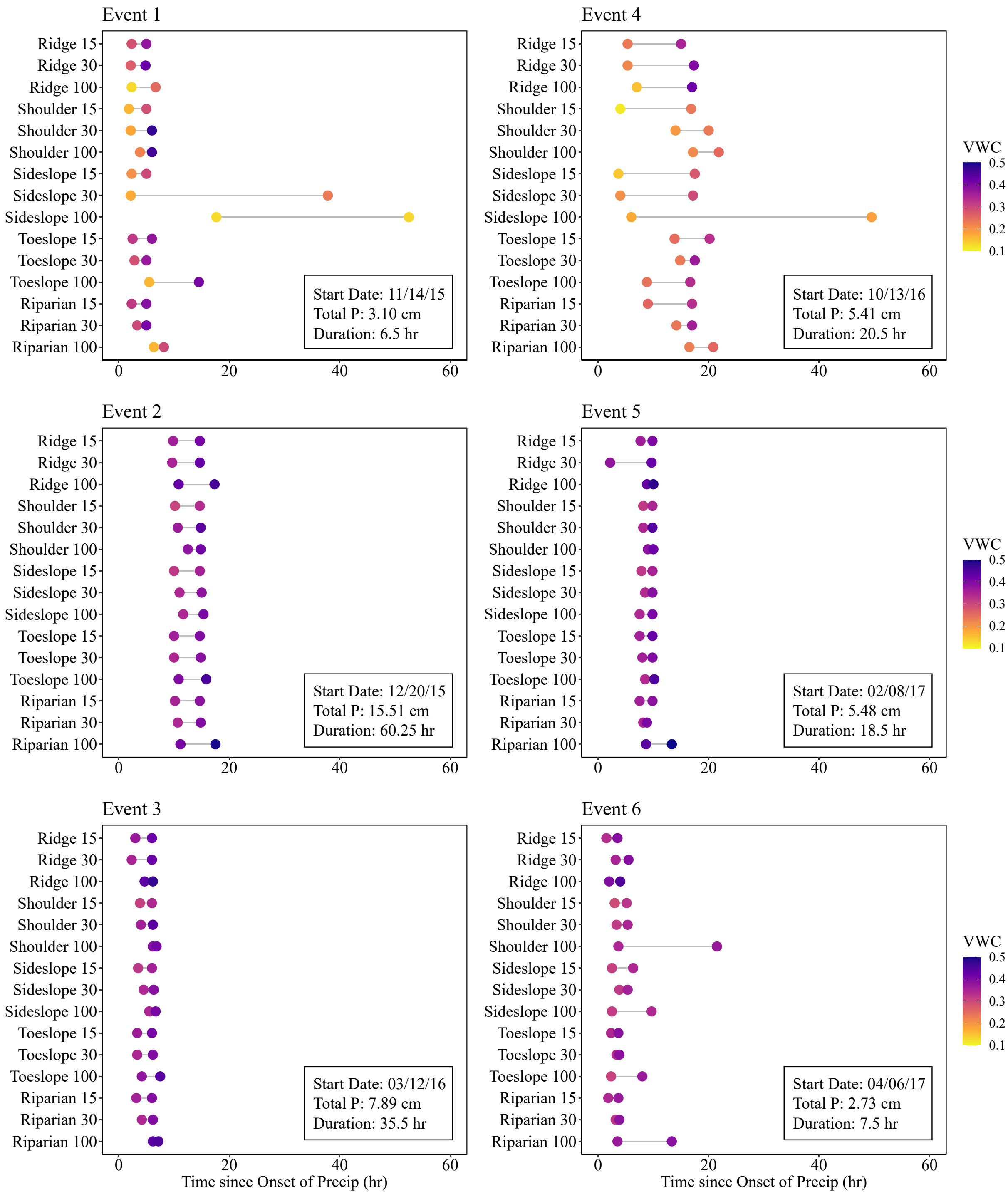

Figure 6. Event metrics for six events occurring in WY16 (left column) and WY17 (right column) including first 2.5 cm event (top), largest event (middle), and last event of season (bottom). The first dot represents the lag time (initial increase of +0.5% in volumetric water content), while the second dot represents the time to peak. The lines connecting the dots represent the lag time to peak. The colors of the dots are associated with the starting soil moisture content and maximum moisture content (second dot). Data are shown for each topographic position and soil depth. Date formats are mm/dd/yy.

Table 4
Soil Moisture Drawdown Metrics by Water Year for Three Soil Depths and Five Topographic Positions in Three Sub-Watersheds of the South Fork Caspar Creek

		WY16					WY17				
Topographic position	Soil depth	Start VWC	Min VWC	Days to min	k	R^2	Start VWC	Min VWC	Days to min	k	R^2
Riparian	15	0.35	0.25	149	−2.0E−03	0.96	0.36	0.23	148	−2.0E−03	0.85
	30	0.33	0.24	154	−2.0E−03	1.00	0.34	0.23	174	−2.0E−03	0.93
	100	0.34	0.23	158	−3.0E−03	0.99	0.38	0.23	175	−2.0E−03	0.78
Toeslope	15	0.38	0.23	149	−3.0E−03	0.98	0.36	0.24	174	−2.0E−03	0.97
	30	0.34	0.23	141	−4.0E−03	0.94	0.35	0.17	149	−5.0E−03	0.91
	100	0.28	0.18	155	−5.0E−03	0.98	0.32	0.21	148	−2.0E−03	0.89
Sideslope	15	0.31	0.14	149	−5.0E−03	0.99	0.33	0.14	166	−6.0E−03	0.98
	30	0.32	0.21	154	−3.0E−03	0.99	0.33	0.20	175	−3.0E−03	0.99
	100	0.31	0.18	155	−4.0E−03	0.98	0.33	0.18	174	−4.0E−03	0.98
Shoulder	15	0.29	0.09	136	−1.0E−02	1.00	0.31	0.09	166	−7.0E−03	0.98
	30	0.31	0.18	137	−5.0E−03	0.99	0.34	0.18	174	−4.0E−03	1.00
	100	0.31	0.21	134	−2.0E−03	0.94	0.38	0.22	175	−3.0E−03	0.96
Ridge	15	0.36	0.21	124	−4.0E−03	0.96	0.35	0.18	174	−4.0E−03	0.97
	30	0.34	0.19	142	−4.0E−03	0.97	0.35	0.22	174	−3.0E−03	0.94
	100	0.37	0.15	142	−5.0E−03	0.87	0.43	0.15	175	−6.0E−03	0.99

Note. k represents the exponential decay term and R^2 is for the best-fit exponential line.

As the wet season progressed, the hillslopes responded more uniformly to events, with shorter lag times and lags to peaks, regardless of the storm characteristics (Figure 6). Soils generally were well above field capacity prior to and during the peak and last events of each year.

4.4. Soil Moisture Drawdown

At most of the topographic positions and soil depths, the period of soil moisture drawdown was longer during the wetter WY17 (168 days) than in WY16 (145 days) (Table 4). Overall, most soils started at a wetter soil moisture content at the beginning of the drawdown period in WY17 versus WY16. About one third of the sites had a lower minimum soil moisture content at the end of the drawdown period in WY16, another third had lower minimum soil moisture in WY17, and the remaining one third of sites reached the same minimum soil moisture content regardless of water year. There was no obvious organization of recession rates across the different soil depths and topographic positions (Figure 7), although ANOVA showed that both depth and position were significant determinants of the recession rates ($p < 0.05$). The steep recession of shallow soils at the shoulder positions was evident in both WY16 and WY17.

5. Discussion

5.1. Organization Into Wet and Dry Moisture States

We found that both vertical and spatial soil moisture patterns at Caspar Creek organized into wet and dry states that were consistent with periods of water excess and deficit, respectively (Figures 2 and 3). Additionally, we found evidence of increasing homogeneity of soil moisture under wet conditions across all depths and topographic positions and increasing variability under drier soil conditions (Figures 3 and 4). Our results broadly support the theory that hillslope soil moisture organizes into two preferred states: (a) A wet state in which soil moisture is driven in part by catchment terrain, resulting in wetter areas deeper in the soil profile and at downslope positions; and (b) a dry state in which patterns in hillslope soil moisture are driven by soil characteristics and the vertical fluxes of evapotranspiration (Famiglietti et al., 1998; Grayson

10.1029/2020WR029170

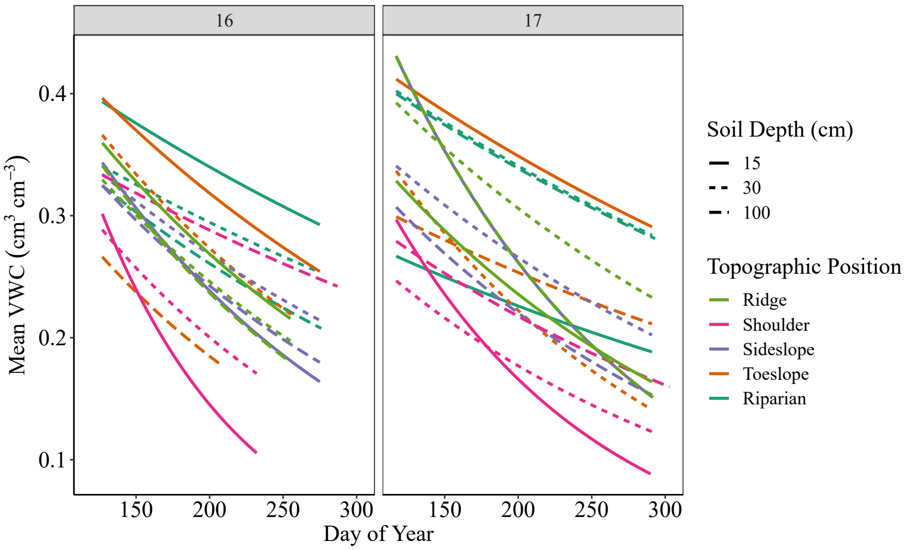

Figure 7. Exponential decay soil moisture drawdown curves for WY16 and WY17 during the dry period. Day of year represents calendar year instead of water year.

et al., 1997). Additionally, our results support previous findings that the spatial and vertical organization of wet and dry moisture states is complex (e.g., Salve et al., 2012). Specifically, we found multiple cases where soil moisture dynamics across depths and topographic positions did not fit our hypotheses. We discuss some of these surprising results in the following sections.

5.2. Wet Ridges

We found that ridges at Caspar Creek during the wet season often were only 3%–5% wetter than topographic positions near the stream channels (i.e., riparian and toeslope sites). Typically, wet season soil moisture is a function of nonlocal topographic characteristics such as hillslope curvature and distance to the stream channel network; these nonlocal controls serve as drivers that predict which portions of the hillslope will remain the wettest (Beven & Kirkby, 1979; Burt & Butcher, 1985; Grayson et al., 1997; Litaor et al., 2008; Tromp-van Meerveld & McDonnell, 2006; Voepel et al., 2011). Indeed, terrain indices such as the topographic wetness index (TWI) and upslope accumulated area (UAA) have been developed and widely used to describe patterns of hillslope wetness and streamflow generation in montane systems underlain by impermeable bedrock or a confining layer (e.g., Beven & Kirkby, 1979; Western et al., 1999). As the highly conductive, thick saprolite layer at our field site can result in deep infiltration, the use of TWI for determining hillslope wetness is likely not appropriate at Caspar Creek despite the spatially intermittent presence of an argillic horizon. Indeed, we ran a simple linear regression analysis to test the relationship between maximum and mean soil moisture during the wet and dry seasons and TWI and UAA, and found no significant results at any soil depths ($\alpha = 0.05$; Figure S1 in the Supporting Information S1). Other studies have similarly found that soil moisture is decoupled from TWI at dry and wet extremes (Tenenbaum et al., 2006). Studies have shown that terrain wetness indices are not universally appropriate in some montane systems (e.g., Jarecke et al., 2021; Keppeler & Brown, 1998; Penna et al., 2009). For instance, at the HJ Andrews Experimental Forest in the Oregon Cascades, it was recently found that hillslope soil moisture was primarily a function of soil properties and not of hillslope topography (Jarecke et al., 2021). Similarly, Penna et al. (2009) found terrain indices alone to be poor predictors in spatial patterns of soil moisture.

The wet ridges at Caspar Creek may have resulted from their relatively gentle surface slopes and deep soil profiles, especially compared to the shoulder and sideslope positions (Table 1). The maximum slope for our ridge sites was 36%, while the maximum slopes were 70% on the shoulder sites and 85% on the sideslope sites. The steeper hillslopes may have resulted in increased interflow from these sites during the wet season, resulting in vertical and lateral drainage and thus lower soil moisture values (Mirus, 2015). For a related study, we installed piezometers to approximately bedrock at each site. The mean depth to bedrock across the three study watersheds was 314 cm for the sideslope, 597 cm for the shoulder, and 616 cm at the ridge positions (Table 1). Thus, the deep soil and saprolite layers at the ridge positions may have enabled deeper infiltration with less lateral flow, thus keeping these positions wetter that the shoulders and sideslopes.

5.3. Wet Season Moisture Dynamics

We hypothesized that the vertical soil moisture variability across the hillslopes would be the lowest during the wet season when water inputs from precipitation are relatively high and losses from evapotranspiration are low. We also thought that positions lower on the hillslope and deeper in the soil profile would exhibit greater overall soil moisture contents than higher topographic positions and shallower soil depths due to the accumulation of saturated subsurface flow at the bottom of the hillslope (interflow) and vertical percolation. Throughout the wet season, increases in soil moisture following individual rain events were noticeable across the entire hillslope (Figure 2), with rapid drainage due to the sandy soil texture and high K_{sat} ($3.8E^{-3}$ to $7.2E^{-2}$ cm s^{-1}). The long duration of high soil moisture during the wet season can furthermore provide connectivity among macropores necessary for well-documented quick streamflow responses to rainfall due to subsurface pipeflow in these sub-watersheds (Keppeler & Brown, 1998; Keppeler et al., 1994; Ziemer & Albright, 1987).

While the uniformly high moisture content during the wet season can be seen in a variety of analyses provided here (e.g., Figures 2–4, Table 3), the response to precipitation events during the wet season also highlights their homogeneity. In general, the different soil depths across all hillslope positions started wet, had a quick but small increase in soil moisture following precipitation, and then rapidly drained following the cessation of rainfall (Figures 2 and 6). Interestingly, the 100 cm soil layers sometimes responded more quickly to rain events than the shallower 30 cm soils, and this was most noticeable in the early season storm events. This is likely indicative of preferential flow pathways that function to route water more efficiently than it is absorbed by the relatively dry soil matrix; preferential flow can also form under high rainfall intensities. Anecdotally, co-located piezometer data from these sites also suggest that shallow groundwater can sometimes respond more quickly to rain events than the soil moisture, which is indicative of preferential flow pathways (Saffarpour et al., 2016). The common occurrence of landslides and unpaved roads in the Caspar Creek watersheds influences the soil moisture dynamics and probably more so during the wetter months when there is greater hydrologic connectivity. Efforts are underway to better understand the influence of these features on hydrologic response in the watersheds.

5.4. High Variability in Deep Soil Moisture

An unexpected finding was the high temporal variability in soil moisture in deeper soils during both the wet and dry seasons (Figure 4). Deeper soils often attenuate rainfall inputs and thereby display more stable moisture conditions over time than shallow soils that are physically closer to precipitation inputs. This has been corroborated by other field studies, which have shown that there is greater temporal stability in soil moisture both in deeper soils (e.g., Williams et al., 2009) and weathered bedrock (Salve et al., 2012). Additionally, there is often an inverse relationship between soil depth and mean volumetric water content, subject to variations in rainfall timing, depth, and intensity (Liang & Chan, 2017; Williams et al., 2009).

The deep soils often started out the wet season at a drier moisture state than the shallower positions, which likely increased the overall variability at these depths. While the clay content of a soil often increases with increasing depth, our soil profiles had only relatively small clay fractions at all depths (Table 2). Thus, the deep, sandy soils at our sites were responding quickly to rain events (Figures 2 and 6) and draining quickly, resulting in greater variability in daily soil moisture than we expected. Given the presence of a deep well-drained saprolite layer, additional sensors deeper in the profile may have captured different dynamics and revealed more stable moisture at greater depths. At Caspar Creek, discontinuous argillic horizons can exist within the upper 2 m of the soil profile and can facilitate the development of preferential flow paths (soil pipes) near stream corridors (Ziemer & Albright, 1987), which could have driven some of the variability in soil moisture at the riparian and toeslope positions. Furthermore, there could have been some influence of groundwater encroachment at the riparian sites, where pore pressures reached within 1 m of the ground surface during the wet season.

5.5. Quick Dry to Wet Transitions in Soil Moisture

The transition from the dry period to the wet period at Caspar Creek occurred rapidly across the hillslopes, with most topographic positions and soil depths starting the water year below field capacity. On average, soils across the hillslope had reached their mean wet season moisture content by late November or early December, after an average of 33 cm of rain had fallen on the watershed. Generally, approximately 20 cm of rainfall is needed to generate the first-of-season "storm" flow at the South Fork Caspar Creek weir (>0.69 m^3/s) but, once the soil profile has been wetted, a new stormflow response occurs with as little as 5 cm of additional precipitation. This is similar to other rainfall-runoff thresholds found in northern California (Sayama et al., 2011).

The soil moisture response to the first large precipitation event of each of the study years was not universal across the hillslope or vertical soil profile, which was not surprising given the difference in antecedent moisture conditions. The first event of WY16 occurred during early recovery from a 3-year drought (12-month standardized precipitation index of −1.37) (Keppeler & Wagenbrenner, 2019), and generally had shorter lag times and lag to peak times across the hillslopes than the first storm of WY17 when the drought had been largely ameliorated (12-month standardized precipitation index of 1.29) (Keppeler & Wagenbrenner, 2019). The WY16 event occurred approximately one month later, was shorter in duration, and had a lower total rainfall than the WY17 event, all of which could explain the differences between the two years (Table S2 in the Supporting Information S1). For both years, the deep sideslope positions had significantly longer lag times and lag to peak times than the other sites (Figure 6). Blume et al. (2009) found similar spatial heterogeneity following precipitation events in sandy volcanic soils, attributing much of the variability across space to preferential flow pathways. Similarly, a large analysis of storm events across watersheds in the southern Appalachian mountains also found that soil moisture responses varied widely depending on hillslope properties, storm characteristics, and antecedent conditions (Singh et al., 2021).

5.6. Variability in Transitions From Wet to Dry Moisture State

The topographic positions and soil depths all drained at statistically unique rates, suggesting that local controls such as vegetation were most important in determining the rate at which soils dried at a particular hillslope position (Figure 7). Despite a lack of similarity among topographic positions and depths, the soil moisture recession rates were similar between the two study years at a given hillslope position and soil depth. The period of drying occurred slowly over the course of five to six months, which was long compared to the rapid wetting of soils during the transition from the dry season to the wet season. A similar pattern of "wet and dry with slow transitions" has been observed at multiple locations in eastern Australia (Grayson et al., 1997; Kalma et al., 1995; Loague, 1992). These transitions have been suggested to be the most complicated in developing hydrologic models and understanding ecohydrological dynamics in a watershed, as many different factors contribute to the observed level of soil moisture at a particular hillslope location and soil depth.

Despite the prolonged period of drying across the hillslopes, the soil moisture content remained relatively high and mean minimum dry season soil moisture was above or at the wilting point at almost all sites (Tables 2 and 3), despite the strong drought at the beginning of the study. The 15 cm depth at the sideslope and shoulder sites did dry below the wilting point. The relative wetness of these hillslopes suggest that this study site might be relatively resistant to drought. Similar results have been found in this region where, even in drought conditions, precipitation is enough to replenish the vegetation-accessible moisture storage (Hahm et al., 2019). It could also be true that our definition of wilting point and field capacity may have been off at the sites, which warrants future investigation. However, it is possible that these hillslopes could dry out more during the summer months if plant transpiration were to increase as a result of increased demand due to warming or reduced fog. Fog is known to enhance plant growth in this region (e.g., Dawson, 1998), yet a corollary study at Caspar Creek found that fog drip was not enough to generate a response in soil moisture in the upper soil profile (Petreshen, *In prep*). The feedbacks between soil moisture and plant transpiration are intrinsically linked, with increased plant demand for water drawing down soil moisture (Dymond et al., 2014) and in return, evapotranspiration being limited by low soil moisture (Jung et al., 2010).

5.7. Vegetation Effects on Dry Season Soil Moisture

In many catchments, plant species and soil textures vary significantly across topographic gradients; these variations may be the primary driver of variable growing season soil moisture dynamics along a hillslope gradient (Breshears et al., 2009; Dymond et al., 2017; Grayson et al., 1997; Moeslund et al., 2013; Tromp-van Meerveld & McDonnell, 2006). Teuling and Troch (2005) demonstrated that soil texture and vegetation can interact to create spatial heterogeneity in soil moisture across a landscape during periods of drying, with increased spatial homogeneity occurring during times of wetness. The controls of soil properties and vegetation can also be dependent upon whether or not soil moisture falls below field capacity (Teuling & Troch, 2005), further complicating the understanding of how soil moisture varies across space and time across a landscape. Our study sites, however, had comparatively homogeneous soil textures regardless of the topographic position. While the soil texture did vary marginally across the study sites, the clay content at any given depth or topographic position only ranged between 3% and 8% (Table 2) and other soil properties were relatively uniform. Moreover, while there were differences in the makeup and relative frequency of vegetation across the study sites, the general plant communities and dominant overstory species were relatively consistent across watersheds (Hammerschmidt, 2020). Riparian sites generally had more biomass as indicated by basal area ($\bar{x} = 30.3$ m^2 ha^{-1}) than the other five topographic positions (basal area ranged from 4.9 to 10.9 m^2 ha^{-1}) (Table S3 in the Supporting Information S1). Riparian sites also had the greatest degree of canopy closure (Table 1), which limits understory evapotranspiration rates (Hammerschmidt, 2020).

In our two study years, there was no significant difference in soil moisture among topographic positions at 30 cm depth, particularly during the dry season (Figure 4). One possible explanation is that the acquisition of soil water by plant roots in this zone resulted in a convergence of mean monthly soil moisture across the hillslopes. Coast redwood, which is the dominant overstory species at Caspar Creek, has deep and wide-spreading lateral roots with no central taproot (Olson et al., 1990). Although the maximum rooting depth of coast redwood is around 250 cm (Karizumi, 1979), field observations suggest that the primary rooting depth of the vegetation in the study-watersheds was <50 cm. During the spring, diurnal fluctuations in soil moisture at the 30 cm depth (data not shown) were more evident than at 15 or 100 cm, possibly suggesting that plant-water uptake was occurring from this mid-profile sampling depth. However, we do not see a more rapid soil moisture decline or lower minimum soil moisture values at these depths (Figure 7; Table 3). A global synthesis of plant rooting depth suggests that the roots of evergreen needle leaf trees are sensitive to the moisture availability in the vertical soil profile (Fan et al., 2017).

As indicated by basal area, the variability in species composition and biomass between our plots likely drives differences in soil drawdown dynamics, this alone cannot explain the convergence of dry season mean soil moisture at 30 cm depth across the five hillslope positions. One possible explanation is niche partitioning of plant roots and water acquisition strategies within the 30 cm rooting zone. Niche partitioning or the process by which different species utilize environmental resources such that they can co-exist, often occurs throughout grassland and forest plant communities (e.g., Chapin et al., 2002; Guderle et al., 2018). In regard to plant-water acquisition from 30 cm soil depth at Caspar Creek, niche partitioning would suggest that different plant communities root efficiently such that growing season soil water is depleted to approximately the same extent along hillslope transects. At Caspar Creek, water use strategies across species and individuals likely also shift across the hillslope positions, especially as fog events enhance summertime water availability at the ridge and shoulder positions to a greater degree than positions at lower elevations.

6. Conclusions

This study investigated the organization of hillslope soil moisture into wet and dry states and the transitions between these two moisture states along a topographic gradient and across soil depths. Previous studies in similar Mediterranean climates have found that soil moisture in the wet season is driven in part by topographically induced factors, while soil moisture in the dry season is highly variable due to its dependence on highly localized vertical transports of water, including inputs from coastal fog. In contrast, we found that mean wet season soil moisture did not follow typical topographic drivers, with ridges retaining wetness at levels similar or above positions nearest to the stream channel. Additionally, we found great variability in deep (100 cm) soil moisture across both wet season and dry seasons, which we attribute to high infiltration with lower lateral movement during the wet season. Soil moisture transition from wet to dry states was a lengthy process (>5 months) and the rate of soil drawdown was highly variable across topographic positions and soil depths, likely due to differences in vegetation and microtopography and slight variations in soil texture across the sites. In contrast, soils uniformly transitioned from dry to wet within 1–2 months. Lastly, we found that mean soil moisture at 30 cm depth was relatively consistent across the topographic gradient, particularly during the dry season. Our results, in conjunction with other recent studies, suggest that there are complex interactions between topography, soil characteristics, vegetation, and seasonal soil moisture dynamics. This has implications for watershed scale modeling and our interpretation of runoff generation mechanisms as site-specific soil, vegetation, and water interactions might be hard to scale up and generalize across landscapes.

Data Availability Statement

Soil moisture data are publicly available via the CUAHSI HydroShare Database (https://doi.org/10.4211/hs.77664f7a07854e17b29557fe308b3dfa) and precipitation data are available through the Forest Service Research Data Archive (https://doi.org/10.2737/RDS-2020-0018-2).

Acknowledgments

Funding and support for this research was provided by the California Department of Forestry and Fire Protection, the USDA Forest Service Pacific Southwest Research Station (PSW), and National Science Foundation (NSF) (NSF-EAR-1807165). We thank Brian Storms, Megan Arnold, and the Caspar Creek Watershed Experiment field team for field and technical assistance. Special thanks to Chris Faubion (PSW) for soil sampling, Ryan Cole (ORISE-PSW), Caroline Ristuccia, and Diane Sutherland (PSW) for processing soil samples, and Shelby Hammerschmidt (PSW) for reviewing data and making maps. Thank you to Dave Longstreth and Patrick Brand (California Geological Survey) for assistance with interpreting the underlying geologic formations at Caspar Creek.

References

Allan, C. J., & Roulet, N. T. (1994). Runoff generation in zero-order Precambrian shield catchments: The stormflow response of a heterogeneous landscape. *Hydrological Processes*, *8*(4), 369–388. https://doi.org/10.1002/hyp.3360080409

Anderson, M. G., & Burt, T. P. (1978). Toward more detailed field monitoring of variable source areas. *Water Resources Research*, *14*(6), 1123–1131. https://doi.org/10.1029/WR014i006p01123

Aulenbach, B. T., & Peters, N. E. (2018). Quantifying climate-related interactions in shallow and deep storage and evapotranspiration in a forested, seasonally water-limited watershed in the southeastern United States. *Water Resources Research*, *54*, 3037–3061. https://doi.org/10.1002/2017WR020964

Baldocchi, D. D., & Xu, L. (2007). What limits evaporation from Mediterranean oak woodlands—The supply of moisture in the soil, physiological control by plants or the demand by the atmosphere? *Advances in Water Resources*, *30*(10), 2113–2122. https://doi.org/10.1016/j.advwatres.2006.06.013

Band, L. E. (1986). Topographic partition of watersheds with digital elevation models. *Water Resources Research*, *22*(1), 15–24. https://doi.org/10.1029/WR022i001p00015

Bell, K. R., Blanchard, B. J., Witczak, M. W., & Schmugge, T. J. (1980). Analysis of surface moisture variations within large field sites. *Water Resources Research*, *16*(4), 796–810. https://doi.org/10.1029/WR016i004p00796

Beven, K. J., & Kirkby, M. J. (1979). Physically based, variable contribution area model of basin hydrology. *Hydrological Sciences Bulletin*, *24*(1), 43–69. https://doi.org/10.1080/02626667909491834

Black, P. E. (1972). Hydrograph responses to geomorphic and precipitation variables. *Journal of Hydrology*, *17*, 309–329. https://doi.org/10.1016/0022-1694(72)90090-x

Blume, T., Zehe, E., & Bronstert, A. (2009). Use of soil moisture dynamics and patterns at different spatio-temporal scales for the investigation of subsurface flow processes. *Hydrology and Earth System Sciences*, *13*, 1215–1234. https://doi.org/10.5194/hess-13-1215-2009

Bréda, N., Granier, A., Barataud, F., & Moyne, C. (1995). Soil water dynamics in an oak stand - I. Soil moisture, water potentials and water uptake by roots. *Plant and Soil*, *172*(1), 17–27. https://doi.org/10.1007/BF00020856

Breshears, D. D., Myers, O. B., & Barnes, F. J. (2009). Horizontal heterogeneity in the frequency of plant-available water with woodland intercanopy-canopy vegetation patch type rivals that occurring vertically by soil depth. *Ecohydrology*, *2*, 503–519. https://doi.org/10.1002/eco.75

Brooks, J. R., Barnard, H. R., Coulombe, R., & McDonnell, J. J. (2010). Ecohydrologic separation of water between trees and streams in a Mediterranean climate. *Nature Geoscience*, *3*(2), 100–104. https://doi.org/10.1038/ngeo722

Burt, T. P., & Butcher, D. P. (1985). Topographic controls of soil-moisture distributions. *Journal of Soil Science*, *36*(3), 469–486. https://doi.org/10.1111/j.1365-2389.1985.tb00351.x

Chapin, F. S., Matson, P. A., Chapin, M. C., & Mooney, H. A. (2002). *Principles of terrestrial ecosystem ecology* (p. 472). Springer.

Cosh, M. H., Jackson, T. J., Moran, S., & Bindlish, R. (2008). Temporal persistence and stability of surface soil moisture in a semi-arid watershed. *Remote Sensing of Environment*, *112*(2), 304–313. https://doi.org/10.1016/j.rse.2007.07.001

Daly, E., Porporato, A., & Rodriguez-Iturbe, I. (2004a). Coupled dynamics of photosynthesis, transpiration, and soil water balance. Part I: Upscaling from hourly to daily level. *Journal of Hydrometeorology*, *5*(3), 546–558. https://doi.org/10.1175/1525-7541(2004)005<0546:CDOPTA>2.0.CO;2

Daly, E., Porporato, A., & Rodriguez-Iturbe, I. (2004b). Coupled dynamics of photosynthesis, transpiration, and soil water balance. Part II: Stochastic analysis and ecohydrological significance. *Journal of Hydrometeorology*, *5*(3), 559–566. https://doi.org/10.1175/1525-7541(2004)005<0559:CDOPTA>2.0.CO;2

Dawson, T. E. (1998). Fog in the California redwood forest: Ecosystem inputs and use by plants. *Oecologia*, *117*, 476–485. https://doi.org/10.1007/s004420050683

Dunne, T., & Black, R. D. (1970). An experimental investigation of runoff production in permeable soils. *Water Resources Research*, *6*(2), 478–490. https://doi.org/10.1029/wr006i002p00478

Dunne, T., Moore, T. R., & Taylor, C. H. (1975). Recognition and prediction of runoff-producing zones in humid regions. *Hydrological Sciences Bulletin*, *20*(3), 305–327.

Dymond, S. F., Bladon, K. D., Keppeler, E., & Wagenbrenner, J. (2021). Caspar Creek experimental watersheds soil moisture dataset. *HydroShare*. https://doi.org/10.4211/hs.77664f7a07854e17b29557fe308b3dfa

Dymond, S. F., Bradford, J. B., Bolstad, P. V., Kolka, R. K., Sebestyen, S. D., & DeSutter, T. M. (2017). Topographic, edaphic, and vegetative controls on plant-available water. *Ecohydrology*, *10*(8), e1897. https://doi.org/10.1002/eco.1897

Dymond, S. F., Kolka, R. K., Bolstad, P. V., & Sebestyen, S. D. (2014). Long-term soil moisture patterns in a Northern Minnesota forest. *Soil Science Society of America Journal*, *78*, S208–S216. https://doi.org/10.2136/sssaj2013.08.0322nafsc

Eamus, D., Boulain, N., Cleverly, J., & Breshears, D. D. (2013). Global change-type drought-induced tree mortality: Vapor pressure deficit is more important than temperature per se in causing decline in tree health. *Ecology and Evolution*, *3*(8), 2711–2729. https://doi.org/10.1002/ece3.664

Famiglietti, J. S., Devereaux, J. A., Laymon, C. A., Tsegaye, T., Houser, P. R., Jackson, T. J., et al. (1999). Ground-based investigation of soil moisture variability within remote sensing footprints during the Southern Great Plains 1997 (SGP97) Hydrology Experiment. *Water Resources Research*, *35*(6), 1839–1851. https://doi.org/10.1029/1999WR900047

Famiglietti, J. S., Rudnicki, J. W., & Rodell, M. (1998). Variability in surface moisture content along a hillslope transect: Rattlesnake Hill, Texas. *Journal of Hydrology*, *210*(1–4), 259–281. https://doi.org/10.1016/S0022-1694(98)00187-5

Famiglietti, J. S., Ryu, D., Berg, A. A., Rodell, M., & Jackson, T. J. (2008). Field observations of soil moisture variability across scales. *Water Resources Research*, *44*(1), 1–16. https://doi.org/10.1029/2006WR005804

Fan, Y., Miguez-Macho, G., Jobbágy, E. G., Jackson, R. B., & Otero-Casal, C. (2017). Hydrologic regulation of plant rooting depth. *Proceedings of the National Academy of Sciences*, 201712381. https://doi.org/10.1073/pnas.1712381114

Goulden, M. L., & Bales, R. C. (2019). California forest die-off linked to multi-year deep soil drying in 2012–2015 drought. *Nature Geoscience*, *12*(8), 632–637. https://doi.org/10.1038/s41561-019-0388-5

Grayson, R. B., Western, A. W., Chiew, F. H. S., & Blöschl, G. (1997). Preferred states in spatial soil moisture patterns: Local and nonlocal controls. *Water Resources Research*, *33*(12), 2897–2908. https://doi.org/10.1029/97WR02174

Guderle, M., Bachmann, D., Milcu, A., Geockele, A., Bechmann, M., Fischer, C., et al. (2018). Dynamic niche partitioning in root water uptake facilitates efficient water use in more divergent grassland plant communities. *Functional Ecology*, *32*, 214–227. https://doi.org/10.1111/1365-2435.12948

Hahm, W. J., Dralle, D. N., Rempe, D. M., Bryk, A. B., Thompson, S. E., Dawson, T. E., & Dietrich, W. E. (2019). Low subsurface water storage capacity relative to annual rainfall decouples Mediterranean plant productivity and water use from rainfall variability. *Geophysical Research Letters*, *46*(12), 6544–6553. https://doi.org/10.1029/2019GL083294

Hammerschmidt, S. (2020). *Understory transpiration rates following stand density reduction in a coast redwood forest*. Retrieved from the University of Minnesota Digital Conservancy https://hdl.handle.net/11299/217771

Henry, N. (1998). Overview of the Caspar Creek watershed study. In R. R. Ziemer technical coordinator. *Proceedings of the conference on coastal watersheds: the Caspar Creek story, 6 May 1998*; Ukiah, California. *(General Tech. Rep. PSW GTR-168* (pp. 1–9). Pacific Southwest Research Station, Forest Service, U.S. Department of Agriculture.

Hills, R. C., & Reynolds, S. G. (1969). Illustrations of soil moisture variability in selected areas and plots of different sizes. *Journal of Hydrology*, *8*, 27–47. https://doi.org/10.1016/0022-1694(69)90029-8

Ivanov, V. Y., Bras, R. L., & Vivoni, E. R. (2008a). Vegetation-hydrology dynamics in complex terrain of semiarid areas: 1. A mechanistic approach to modeling dynamic feedbacks. *Water Resources Research*, *44*(3), W03429. https://doi.org/10.1029/2006WR005588

Ivanov, V. Y., Bras, R. L., & Vivoni, E. R. (2008b). Vegetation-hydrology dynamics in complex terrain of semiarid areas: 2. Energy-water controls of vegetation spatiotemporal dynamics and topographic niches of favorability. *Water Resources Research*, *44*(3), 1–20. https://doi.org/10.1029/2006WR005595

Jarecke, K. M., Bladon, K. D., & Wondzell, S. M. (2021). The influence of local and nonlocal factors on soil water content in a steep forested catchment. *Water Resources Research*, *57*(5), e2020WR028343. https://doi.org/10.1029/2020wr028343

Johnstone, J. A., & Dawson, T. E. (2010). Climatic context and ecological implications of summer fog decline in the coast redwood region. *Proceedings of the National Academy of Sciences of the United States of America*, *107*(10), 4533–4538. https://doi.org/10.1073/pnas.0915062107

Jung, M., Reichstein, M., Ciais, P., Seneviratne, S. I., Sheffield, J., Goulden, M. L., et al. (2010). Recent decline in the global land evapotranspiration trend due to limited moisture supply. *Nature*, *467*(7318), 951–954. https://doi.org/10.1038/nature09396

Kalma, J. D., Bates, B. C., & Woods, R. A. (1995). Predicting catchment-scale soil moisture states with limited field measurements. *Hydrological Processes*, *9*, 445–467. https://doi.org/10.1002/hyp.3360090315

Karizumi, N. (1979). Monograph - Root system forms and distributions of individual trees in Japan (in Japanese). Seibundo Shinkosha Publishing Co. Ltd. Retrieved from https://www.cabdirect.org/cabdirect/abstract/19870618641

Keppeler, E. T., & Brown, D. (1998). Subsurface drainage processes and management impacts. In R. R. Ziemer (Ed.), *Proceedings of the conference on coastal watersheds: The Caspar Creek story, general technical report PSW GTR-168* (Vol. *2*, pp. 25–34). U.S. Forest Service Pacific Southwest Research Station.

Keppeler, E., & Wagenbrenner, J. (2019). The role of drought in the hydrologic response of a managed coast redwood watershed. In *6th Interagency Conference on Research in the Watersheds* (pp. 10–13).

Keppeler, E. T., & Ziemer, R. R. (1990). Logging effects on streamflow: Water yield and summer low flows at Caspar Creek in Northwestern California. *Water Resources Research*, *26*(7), 1669–1679. https://doi.org/10.1029/wr026i007p01669

Keppeler, E. T., Ziemer, R. R., & Cafferata, P. H. (1994). Changes in soil moisture and pore pressure after harvesting a forested hillslope in northern California. In R. A. Marston, & V. R. Hasfutehr (Eds.), *Proceedings of the annual summer sympoisum of the American water resources association: Effects of human-induced changes on hydrologic systems. June 26–29, Jackson Hole, WY* (pp. 2015–2214). American Water Resources Association.

Klein, T., Rotenberg, E., Cohen-Hilaleh, E., Raz-Yaseef, N., Tatarinov, F., Preisler, Y., et al. (2014). Quantifying transpirable soil water and its relations to tree water use dynamics in a water-limited pine forest. *Ecohydrology*, *7*(2), 409–419. https://doi.org/10.1002/eco.1360

Klos, P. Z., Goulden, M. L., Riebe, C. S., Tague, C. L., O'Geen, A. T., Flinchum, B. A., et al. (2018). Subsurface plant-accessible water in mountain ecosystems with a Mediterranean climate. *Wiley Interdisciplinary Reviews: Water*, *5*(3), e1277. https://doi.org/10.1002/wat2.1277

Lawrence, J. E., & Hornberger, G. M. (2007). Soil moisture variability across climate zones. *Geophysical Research Letters*, *34*, L20402. https://doi.org/10.1029/2007gl031382

Liang, W. L., & Chan, M. C. (2017). Spatial and temporal variations in the effects of soil depth and topographic wetness index of bedrock topography on subsurface saturation generation in a steep natural forested headwater catchment. *Journal of Hydrology*, *546*, 405–418. https://doi.org/10.1016/j.jhydrol.2017.01.033

Link, P., Simonin, K., Maness, H., Oshun, J., Dawson, T. E., & Fung, I. (2014). Species differences in the seasonality of evergreen tree transpiration in a Mediterranean climate: Analysis of multiyear, half-hourly sap flow observations. *Water Resources Research*, *50*, 1869–1894. https://doi.org/10.1002/2013wr014023

Lisle, T. E. (1989). Correction to "Sediment transport and resulting deposition in spawning gravels, north coastal California" by Thomas E. Lisle. *Water Resources Research*, *25*(10), 2285–2285. https://doi.org/10.1029/WR025i010p02285

Litaor, M. I., Williams, M., & Seastedt, T. R. (2008). Topographic controls on snow distribution, soil moisture, and species diversity of herbaceous alpine vegetation, Niwot Ridge, Colorado. *Journal of Geophysical Research*, *113*, 1–10. https://doi.org/10.1029/2007JG000419

Loague, K. (1992). Soil water content at R-5 Part 2. Impact of antecedent conditions on rainfall-runoff simulations. *Journal of Hydrology*, *139*(1–4), 253–261. https://doi.org/10.1016/0022-1694(92)90205-a

Miller, B. A., & Schaetzl, R. J. (2015). Digital classification of hillslope position. *Soil Science Society of America Journal*, *79*, 132–145. https://doi.org/10.2136/sssaj2014.07.0287

Mirus, B. B. (2015). Evaluating the importance of characterizing soil structure and horizons in parameterizing a hydrologic process model. *Hydrological Processes*, *29*, 461–4623. https://doi.org/10.1002/hyp.10592

Moeslund, J. E., Arge, L., Bøcher, P. K., Dalgaard, T., OdgaardNygaard, M. V. B., & Svenning, J. C. (2013). Topographically controlled soil moisture is the primary driver of local vegetation patterns across a lowland region. *Ecosphere*, *4*(7), 1–26. https://doi.org/10.1890/ES13-00134.1

Moore, I. D., Burch, G. J., & Mackenzie, & D. H. (1988). Topographic effects on the distribution of surface water and the location of ephemeral gullies. *Transactions of the ASAE*, *31*(4), 1098–1107. https://doi.org/10.13031/2013.30829

Naseri, M., Iden, S. C., Richter, N., & Durner, W. (2019). Influence of stone content on soil hydraulic properties: Experimental investigation and test of existing model concepts. *Vadose Zone Journal*, *18*(1), 1–10. https://doi.org/10.2136/vzj2018.08.0163

Nyberg, L. (1996). Spatial variability of soil water content in the covered catchment at Gårdsjön, Sweden. *Hydrological Processes*, *10*(1), 89–103. https://doi.org/10.1002/(SICI)1099-1085(199601)10:1<89::AID-HYP303>3.0.CO;2-W

Oishi, A. C., Oren, R., Novick, K. A., Palmroth, S., & Katul, G. G. (2010). Interannual invariability of forest evapotranspiration and its consequence to water flow downstream. *Ecosystems*, *13*(3), 421–436. https://doi.org/10.1007/s10021-010-9328-3

Olson, D. F., Roy, D. F., & Walters, G. A. (1990). Sequoia sempervirens. In R. M. Burns, & B. H. Honkala (Eds.), *Silvics of North America* (Vol. *1*, pp. 541–551). USDA Forest Service Agriculture Handbook 654.

Orth, R., & Seneviratne, S. I. (2013). Propagation of soil moisture memory to streamflow and evapotranspiration in Europe. *Hydrology and Earth System Sciences*, *17*(10), 3895–3911. https://doi.org/10.5194/hess-17-3895-2013

Penna, D., Borga, M., Norbiato, D., & Dalla Fontana, G. (2009). Hillslope scale soil moisture variability in a steep alpine terrain. *Journal of Hydrology*, *364*, 311–327. https://doi.org/10.1016/j.jhydrol.2008.11.009

Penna, D., Brocca, L., Borga, M., & Dalla Fontana, G. (2013). Soil moisture temporal stability at different depths on two alpine hillslopes during wet and dry periods. *Journal of Hydrology*, *477*, 55–71. https://doi.org/10.1016/j.jhydrol.2012.10.052

Pierce, D. W., Kalansky, J. F., Cayan, D. R. & Scripps Institution of Oceanography. (2018). *Climate, drought, and sea level rise scenarios for California's fourth climate change assessment*. California's Fourth Climate Change Assessment (Publication Number: CN-RA-CEC-2018-006). California Energy Commission.

Price, A. G., & Bauer, B. O. (1984). Small-scale heterogeneity and soil moisture variability in the unsaturated zone. *Journal of Hydrology*, *70*, 277–293. https://doi.org/10.1016/0022-1694(84)90127-6

Reid, L. M., Dewey, N. J., Lisle, T. E., & Hilton, S. (2010). The incidence and role of gullies after logging in a coastal redwood forest. *Geomorphology*, *117*(1–2), 155–169. https://doi.org/10.1016/j.geomorph.2009.11.025

Reynolds, S. G. (1970). The gravimetric method of soil moisture determination Part III An examination of factors influencing soil moisture variability. *Journal of Hydrology*, *11*(3), 288–300. https://doi.org/10.1016/0022-1694(70)90068-5

Rittiman, C. A. & Thorson, T. (2006). Soil survey of Mendocino County, California, western part. U.S. Department of Agriculture, Natural Resources Conservation Service. p 456.

Robeson, S. M. (2015). Revisiting the recent California drought as an extreme value. *Geophysical Research Letters*, *42*, 6771–6779. https://doi.org/10.1002/2015GL064593

Rodriguez-Iturbe, I., D'Odorico, P., Porporato, A., & Ridolfi, L. (1999). On the spatial and temporal links between vegetation, climate, and soil moisture. *Water Resources Research*, *35*(12), 3709–3722. https://doi.org/10.1029/1999WR900255

Ruhe, R. V., & Walker, P. H. (1968). Hillslope models and soil formation: I. Open systems. In *Transactions of the 9th international congress of soil science* (Vol. *4*, pp. 551–560). International Soil Science Society.

Saffarpour, S., Western, A. W., Adams, R., & McDonnell, J. J. (2016). Multiple runoff processes and multiple thresholds control agricultural runoff generation. *Hydrology and Earth System Sciences*, *20*, 4525–4545. https://doi.org/10.5194/hess-20-4525-2016

Salve, R., Rempe, D. M., & Dietrich, W. E. (2012). Rain, rock moisture dynamics, and the rapid response of perched groundwater in weathered, fractured argillite underlying a steep hillslope. *Water Resources Research*, *48*(11), 1–25. https://doi.org/10.1029/2012WR012583

Saxton, K. E., Rawls, W. J., Romberger, J. S., & Papendick, R. I. (1986). Estimating generalized soil-water characteristics from Texture. *Soil Science Society of America Journal*, *50*(4), 1031–1036. https://doi.org/10.2136/sssaj1986.03615995005000040054x

Sayama, T., Mcdonnell, J. J., Dhakal, A., & Sullivan, K. (2011). How much water can a watershed store? *Hydrological Processes*, *25*, 3899–3908. https://doi.org/10.1002/hyp.8288

Schmugge, T. J., & Jackson, T. J. (1996). Soil moisture variability. In J. B. Stewart, E. T. Engman, A. Feddes, & Y. Kerr (Eds.), *Scaling up in hydrology using remote sensing* (pp. 183–192). John Wiley & Sons.

Singh, N. K., Emanuel, R. E., McGlynn, B. L., & Miniat, C. F. (2021). Soil moisture responses to rainfall: Implications for runoff generation. *Water Resources Research*, *57*(9), 1–17. https://doi.org/10.1029/2020WR028827

Spittler, T. E. (1995). Pilot monitoring program: Geologic input for the hillslope component. Unpublished report. Prepared for the California Department of Forestry and Fire Protection, contract no. 8CA38400, Sacramento, CA. p 16. Retrieved from https://www.fs.fed.us/psw/publications/4351/PMP.pdf

Sprenger, M., Llorens, P., Cayuela, C., Gallart, F., & Latron, J. (2019). Mechanisms of consistently disjunct soil water pools over (pore) space and time. *Hydrology and Earth System Sciences*, *23*(6), 2751–2762. https://doi.org/10.5194/hess-23-2751-2019

Tague, C. L., & Band, L. E. (2004). RHESSys: Regional hydro-ecologic simulation system—An object-oriented approach to spatially distributed modeling of carbon, water, and nutrient cycling. *Earth Interactions*, *8*(19), 1–42. https://doi.org/10.1175/1087-3562(2004)8<1:rrhsso>2.0.co;2

Tague, C. L., Moritz, M., & Hanan, E. (2019). The changing water cycle: The eco-hydrological impacts of forest density reduction in Mediterranean (seasonally dry) regions. *WIREs Water*, *6*, e1350. https://doi.org/10.1002/wat2.1350

Tenenbaum, D. E., Band, L. E., Kenworthy, S. T., & Tague, C. L. (2006). Analysis of soil moisture patterns in forested and suburban catchments in Baltimore, Maryland, using high-resolution photogrammetric and LIDAR digital elevation datasets. *Hydrological Processes*, *20*, 219–240. https://doi.org/10.1002/hyp.5895

Teuling, A. J., & Troch, P. A. (2005). Improved understanding of soil moisture variability dynamics. *Geophysical Research Letters*, *32*(5), 1–4. https://doi.org/10.1029/2004gl021935

Thornthwaite, C. W. (1948). An approach toward a rational classification of climate. *Geographical Review*, *38*(1), 55–94. https://doi.org/10.2307/210739

Tromp-van Meerveld, H. J., & McDonnell, J. J. (2006). On the interrelations between topography, soil depth, soil moisture, transpiration rates and species distribution at the hillslope scale. *Advances in Water Resources*, *29*(2), 293–310. https://doi.org/10.1016/j.advwatres.2005.02.016

van Genuchten, M. T. (1980). A closed form equation for predicting the hydraulic conductivity of unsaturated soils. *Soil Science Society of America Journal*, *44*, 892–898. https://doi.org/10.2136/sssaj1980.03615995004400050002x

Vertessy, R. A., Hatton, T. J., O'Shaughnessy, P. J., & Jayasuriya, M. D. A. (1993). Predicting water yield from a mountain ash forest catchment using a terrain analysis based catchment model. *Journal of Hydrology*, *150*(2–4), 665–700. https://doi.org/10.1016/0022-1694(93)90131-R

Voepel, H., Ruddell, B., Schumer, R., Troch, P. A., Brooks, P. D., Neal, A., et al. (2011). Quantifying the role of climate and landscape characteristics on hydrologic partitioning and vegetation response. *Water Resources Research*, *47*(8), 1–13. https://doi.org/10.1029/2010WR009944

Warren, J. M., Meinzer, F. C., Brooks, J. R., & Domec, J. C. (2005). Vertical stratification of soil water storage and release dynamics in Pacific Northwest coniferous forests. *Agricultural and Forest Meteorology*, *130*(1–2), 39–58. https://doi.org/10.1016/j.agrformet.2005.01.004

Westerling, A. L., & Bryant, B. P. (2007). Climate change and wildfire in California. *Climatic Change*, *87*, 231–249. https://doi.org/10.1007/s10584-007-9363-z

Western, A. W., & Blöschl, G. (1999). On the spatial scaling of soil moisture. *Journal of Hydrology*, *217*, 203–224. https://doi.org/10.1016/s0022-1694(98)00232-7

Western, A. W., & Grayson, R. B. (1998). The Tarrawarra data set: Soil moisture patterns, soil characteristics, and hydrological flux measurements. *Water Resources Research*, *34*(10), 2765–2768. https://doi.org/10.1029/98WR01833

Western, A. W., Grayson, R. B., Blöschl, G., Willgoose, G. R., & McMahon, T. A. (1999). Observed spatial organization of soil moisture and its relation to terrain indices. *Water Resources Research*, *35*(3), 797–810. https://doi.org/10.1029/1998WR900065

Wigmosta, M. S., Vail, L. W., & Lettenmaier, D. P. (1994). A distributed hydrology-vegetation model for complex terrain. *Water Resources Research*, *30*(6), 1665–1679. https://doi.org/10.1029/94WR00436

Wilke, C. O. (2020). *Package 'ggridges': Ridgeline plots in "ggplot2." R package*. Retrieved from https://wilkelab.org/ggridges/

Williams, C. J., Mcnamara, J. P., & Chandler, D. G. (2009). Controls on the temporal and spatial variability of soil moisture in a mountainous landscape: The signature of snow and complex terrain. *Hydrology and Earth System Sciences*, *13*, 1325–1336. https://doi.org/10.5194/hess-13-1325-2009

Yuan, W., Zheng, Y., Piao, S., Ciais, P., Lombardozzi, D., Wang, Y., et al. (2019). Increased atmospheric vapor pressure deficit reduces global vegetation growth. *Science Advances*, *5*(8), 1–13. https://doi.org/10.1126/sciadv.aax1396

Zehe, E., Graeff, T., Morgner, M., Bauer, A., & Bronstert, A. (2010). Plot and field scale soil moisture dynamics and subsurface wetness control on runoff generation in a headwater in the Ore Mountains. *Hydrology and Earth System Sciences*, *14*(6), 873–889. https://doi.org/10.5194/hess-14-873-2010

Ziemer, R. R., & Albright, J. S. (1987). Subsurface pipeflow dynamics of north-coastal California swale systems. In R. Beschta, T. Blinn, G. E. Grant, F. J. Swanson, & G. G. Ice (Eds.), *Erosion and sedimentation in the Pacific Rim, Proceedings of the corvallis symposium* (pp. 71–80). International Association of Hydrological Sciences Publication No. 165.